Coordination Chemistry Reviews 441 (2021) 213976

Contents lists available at ScienceDirect

Coordination Chemistry Reviews

journal homepage: www.elsevier.com/locate/ccr

Review

Dehaloperoxidase: An enzymatic Swiss army knife

Talita Malewschik, Reza A. Ghiladi *

Department of Chemistry, North Carolina State University, Raleigh, NC 27695-8204, United States

ARTICLE INFO

Article history:
Received 4 January 2021
Accepted 11 April 2021

Keywords:
Dehaloperoxidase
Peroxygenase enzymes
Hydrogen peroxide dependent oxidation
Structure-function relationship

ABSTRACT

The hemoglobin from the marine worm *Amphitrite ornata* has been found to possess multiple enzymatic activities in addition to its O_2-transport function. Named dehaloperoxidase (DHP), this globin employs four mechanisms for substrate oxidation as a defense mechanism against toxic metabolites, spanning electron- (peroxidase and oxidase) and O-atom (peroxygenase and oxygenase) transfer. As such, DHP can be defined as a multifunctional catalytic hemoglobin. Given that its peroxidase function is already well established in the literature, this review aims to provide further structural and mechanistic details into the other three activities performed by DHP, with a particular emphasis on its peroxygenase activity.

Contents

Abbreviations: 2-NP, 2-nitrophenol; 2,4-DNP, 2,4-dinitrophenol; 2,4,6-TBP, 2,4,6-tribromophenol; 2,4,6-TCP, 2,4,6-trichlorophenol; 2,4,6-TNP, 2,4,6-trinitrophenol; 4-Br-C, 4-bromo-*o*-cresol; 4-BP, 4-bromophenol; 4-NC, 4-nitrocatechol; 4-NP, 4-nitrophenol; 5-Br-I, 5-bromoindole; AA, amino acid; Compound I, two-electron oxidized heme cofactor compared to the ferric form, commonly referred to as iron(IV)-oxo porphyrin π-cation radical [(Por$^{\bullet+}$)Fe(IV)=O AA]; Compound II, one-electron oxidized heme cofactor when compared to the ferric form [(Por)Fe(IV)=O or (Por)Fe(IV)–OH AA]; Compound ES, two-electron-oxidized state containing both a ferryl center and an amino acid (tryptophanyl or tyrosyl) radical, analogous to Compound ES in cytochrome *c* peroxidase [(Por)Fe(IV)=O $^{\bullet}$AA]; *Agrocybe aegerita* unspecific peroxygenase, (*Aae*UPO); CPO, chloroperoxidase; DHP, dehaloperoxidase; DMPO, 5,5-dimethyl-1-pyrroline N-oxide; DMSO, dimethyl sulfoxide; EPA, Environmental Protection Agency; HRP, horseradish peroxidase; IDO1, human indoleamine 2,3-dioxygenase; Mb, myoglobin; NDO, naphthalene 1,2-dioxygenase; 3H-DMI, 3-hydroxy-2,3-dimethylindole; *o*-AAP, *o*-acetaminoacetophenone; RFQ-EPR, rapid-freeze-quench electron paramagnetic resonance; SET, single electron transfer; SFX, serial femtosecond crystallography; SOD, superoxide dismutase; UPO, unspecific peroxygenase; WT, wild-type.

* Corresponding author.
E-mail address: reza_ghiladi@ncsu.edu (R.A. Ghiladi).

https://doi.org/10.1016/j.ccr.2021.213976
0010-8545/

1. Introduction

The segmented marine worm *Amphitrite ornata* coinhabits benthic ecosystems with other organisms that secret toxic halogenated metabolites as a defense mechanism. In order to survive such harsh environments, *A. ornata* employs its hemoglobin, named dehaloperoxidase (DHP), in the detoxification of these substances [1–4]. DHP is a catalytic globin, a term that was first coined by Lebioda and coworkers [5] after the first identified oxidative function of DHP, peroxidase activity, was discovered in 1996 for the H_2O_2-dependent oxidative dehalogenation of halophenols [2,5]. The substrate scope of DHP has been expanded to include methoxyphenols (guaiacols) and methylphenol (cresols), which were also found to be oxidized via this peroxidase activity (Fig. 1, red and purple) [6,7]. More recently, three additional oxidative activities were discovered for DHP: peroxygenase [8], oxidase [8] and oxygenase (McCombs, dissertation 2017) [9]. The peroxygenase function of DHP, first described in 2014 for the oxidation of haloindoles [8], is also employed in the oxidation of nitrophenols [10], pyrroles [11] and cresols [7] (Fig. 1, blue and purple). The peroxidase function of DHP has been thoroughly investigated and reported in the literature [12–37], thus the purpose of this review is to focus on the more recently identified functions for DHP and more specifically, its peroxygenase function.

1.1. Dehaloperoxidase overview

The *A. ornata* benthic environment is coinhabited by organisms such as *Notomastus lobatus* (Polychaeta) and *Saccoglossus kowalewskyi* (Hemichordata) that release high levels of toxic halogenated aromatic compounds as repellents against predation [2,3]. While living under the umbrella of protection of its neighbors' chemical defense mechanisms, *A. ornata* employs its hemoglobin, DHP, as a biocatalyst to oxidize these repellents, thus enabling it to survive in these harsh environmental conditions [3–5,38–40]. The reaction for which DHP became known as a catalytic globin is the oxidative dehalogenation of 2,4,6-trihalophenol (2,4,6-TXP) yielding the corresponding 2,6-dihalo-1,4-benzoquinone (2,6-DXQ) (Fig. 2, top) [2].

Structural and spectroscopic efforts were employed to understand and elucidate the peroxidase mechanism of the DHP-catalyzed oxidation of halophenols, and it was determined that the peroxidase catalytic cycle of DHP follows the general one proposed by Poulos and Kraut for heme peroxidases [41,42]: the ferric form of the enzyme binds to hydrogen peroxide, and heterolytic cleavage of the O-O bond is assisted by the distal histidine (H55), leading to the formation of Compound I, a highly reactive iron (IV)-oxo center with a porphyrin π -cation radical [(Por$^{\bullet+}$)Fe^{IV}=O AA] species (AA = amino acid). In the catalytic cycle of DHP, Compound I was found to be short-lived [15], yielding Compound ES, [(Por)Fe^{IV}=O $^{\bullet}$AA] after internal electron transfer with a local amino acid residue (i.e., Tyr34, Tyr38 or Tyr28) [18,25,33]. This two-electron oxidized species reacts with a substrate molecule in two consecutive one-electron steps [34], with Compound II [(Por)Fe^{IV}=O AA] as an intermediate [19], returning the enzyme to its ferric resting state. With regards to the substrate, once the phenoxyl radical is formed (Fig. 2**, bottom**), it has been suggested that radical disproportionation leads to carbocation formation, which then rearranges to form the quinone product upon addition of solvent water [14]. Finally, it has been shown that the 2,6-DXQ product undergoes a spontaneous, albeit slow, non-enzymatic oxidation, giving rise to 3-hydroxy-2,6-dihaloquinone (2,6-DXQOH) [37].

Structurally DHP has a 3-on-3 α-helical structure, a known fold for globins, and thus it is characterized as such according to the SCOP database (Structural Classification of Proteins), even though it bears little sequence homology when compared to other known globins [4,5,22,43,44]. The first crystal structure of DHP (PDB: 1EW6) was reported by Lebioda and coworkers in 2000 [43], which reveals that the distal histidine (H55), located on helix E of the

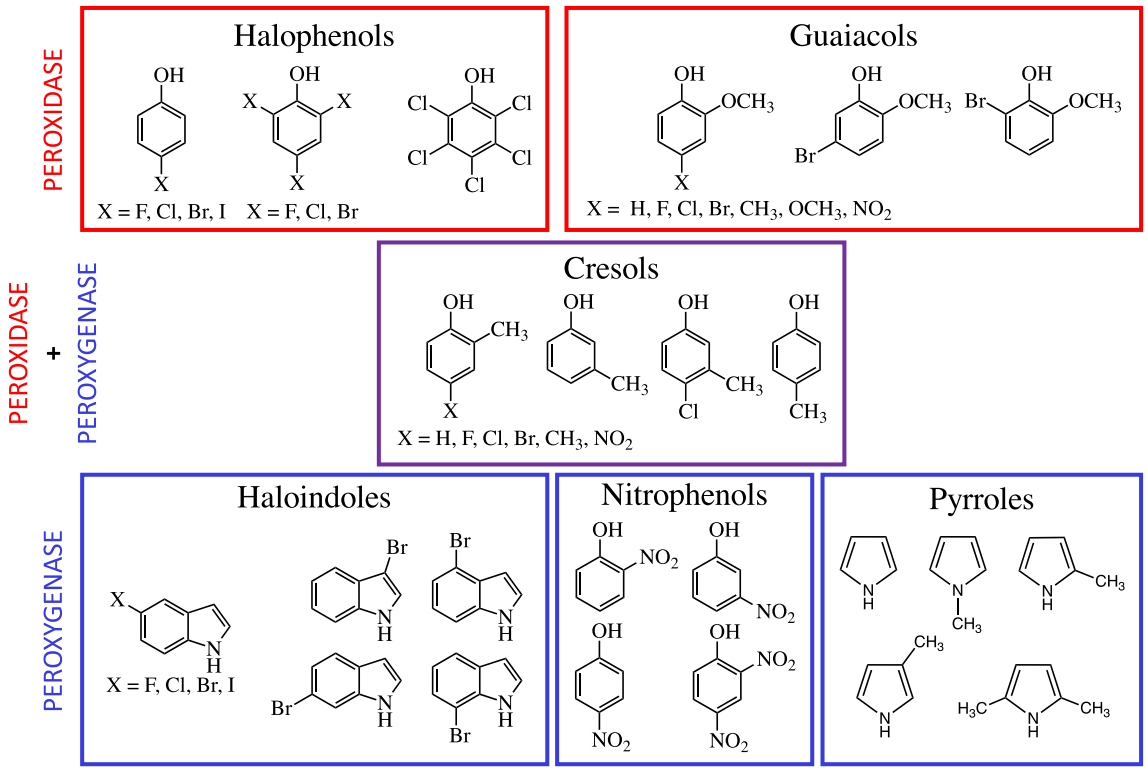

Fig. 1. Substrate scope of dehaloperoxidase showing the peroxidase (red) and peroxygenase (blue) activities employed in substrate oxidation.

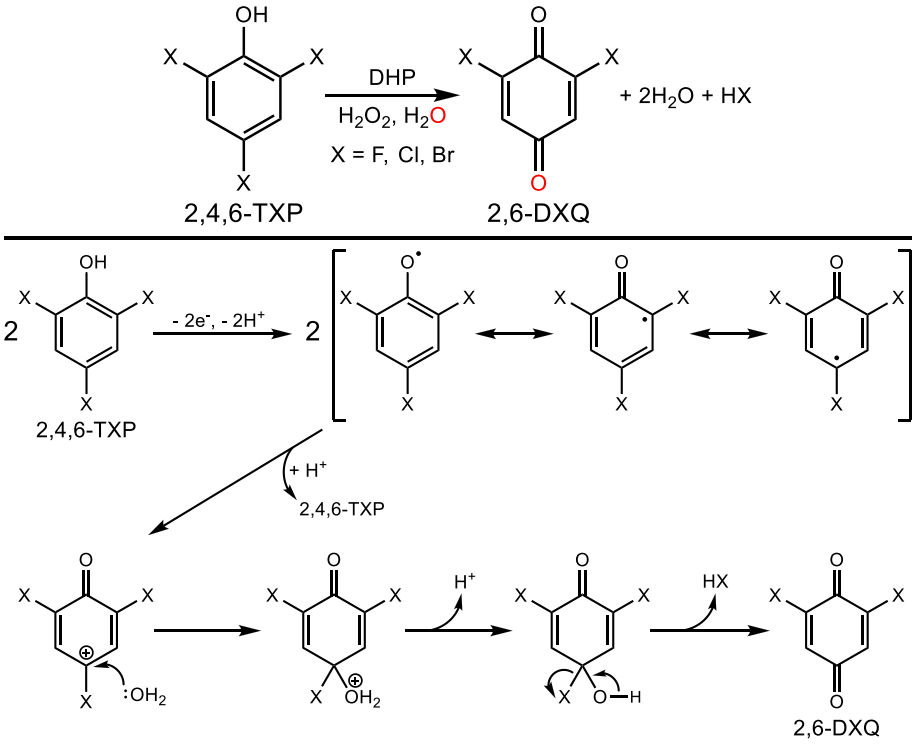

Fig. 2. Top: Peroxidase activity of DHP in the oxidative dehalogenation of 2,4,6-trihalophenol (2,4,6-TXP) into its corresponding 2,6-dihalo-1,4-benzoquinone (2,6-DXQ). Bottom: Possible pathway for product formation, . adapted from [14,37]

structure, plays a major role in the catalytic process and displays an increased flexibility compared to other globins [18,23,43,45,46]. In subsequent functional and structural studies, residues L100, F21, F24, F35, V59 and F60 were found to form a hydrophobic cavity, named the Xe1 binding distal pocket (Fig. 3**A**) [47], that accommodates and interacts with substrates such as halophenols [2,17,20,21,26,34,35,48], haloindoles [8,49], nitrophenols [10], azoles [50], guaiacols [6] and cresols [7]. Residues Y38, T56 [51] and H55 are often found to form stabilizing hydrogen bonding interactions with the substrates in the pocket of DHP (Fig. 3B). The proximal side of the protoporphyrin IX cofactor is stabilized by a proximal histidine (H89), which in conjunction with the backbone carbonyl oxygen of L83, forms a Leu-His-Fe catalytic triad, in comparison to the commonly known Asp-His-Fe triad of classic peroxidases [41,52].

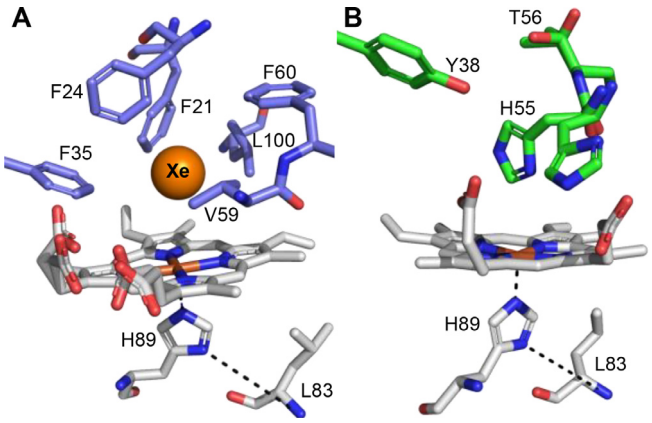

Fig. 3. Relevant amino acid residues in the distal and proximal sides of the heme cofactor in the enzyme dehaloperoxidase A) hydrophobic amino acid residues that constitute the Xe1 binding pocket (PDB: 3MOU), and B) residues responsible for hydrogen bonding interactions with substrates (PDB: 6ONX).

1.2. Heme peroxygenase enzymes

Peroxygenases, a class of enzymes that employ peroxide as the O-atom source for oxyfunctionalization of small molecules, have been increasingly investigated for their substrate promiscuity and versatility. They perform a variety of different oxidative reactions, such as the hydroxylation and epoxidation of aromatic, linear and cyclic alkanes and alkenes, sulfoxidation and N-oxygenation, dechlorination and halide oxidation, amongst others [53–62]. A notable example of a peroxygenase enzyme is the fungal unspecific peroxygenase (UPO), also referred to as aromatic peroxygenases (APOs), which exhibits high catalytic activity and specificity using Mg^{2+} ions as a cofactor. The hydroxylation of naphthalene, shown to proceed via an epoxide intermediate, was the first reaction to be identified for UPOs [53–56,63–68]. UPOs only require H_2O_2 as a co-substrate for catalytic turnover, and they are independent from NAD(P)H or electron transfer chains due to the fact that they are extracellular proteins [54,68], in contrast with the super family of cytochrome P450 enzymes. The P450 class of enzymes are known monooxygenases and their catalytic cycle is O_2 and NAD(P)H-dependent, however they can also employ hydrogen peroxide as an oxidant, where the catalytic cycle proceeds via the "peroxide shunt" pathway [59,69]. One example of a P450-peroxygenase enzyme is the CYP152 family of bacterial cytochromes, such as CYP152A1 ($P450_{BS\beta}$) and B1($P450_{SP\alpha}$), which catalyzes the hydroxylation of fatty acids in the presence of hydrogen peroxide [53,57–61,70–72].

In general, structural differences between peroxidases and peroxygenases impact their reactivity with substrates, where the main difference is the proximal ligand: histidine for peroxidases and cysteine for peroxygenases (UPOs and cytochrome P450s). In addition, in peroxidases there is a local aspartate residue at the proximal

side that contributes to the formation and stabilization of the ferryl active species by interacting with the histidine, which constitutes the catalytic triad (Asp-His-Fe) mentioned above and is shown for horseradish peroxidase (HRP) in Fig. 4**A** [41,42,73–75]. In unspecific peroxygenases, this triad is characterized by a highly conserved PCP motif (proline-cysteine-proline) that has been found to be essential for catalytic activity (Fig. 4B) [56,65,66,68]. At the distal side, the presence of general acid-base catalytic residues, such as histidine, aspartic acid and glutamic acid (Fig. 4A and B), can impact the activation of hydrogen peroxide, leading to the formation of the active ferryl species [41,42,73,76]. In the case of P450s, three natural bacterial enzymes, namely $P450_{BS\beta}$, $P450_{SP}\alpha$ and $P450_{CLA}$, have been identified and found to perform the hydroxylation of fatty acids in the presence of H_2O_2. Their active site does not contain the "general" acid-base residues, so instead the carboxylic acid group of the fatty acyl acid substrate, shown as palmitic acid in Fig. 4**C**, interacts with the guanidinium moiety of a local arginine residue, creating a salt bridge. This is considered to be the first step of the H_2O_2-dependent catalytic cycle and it is referred to as a "substrate-assisted activation mechanism" [57]. In addition, short-alkyl-chain carboxylic acids (C4-C10) were found to "trick" $P450_{BS\beta}$ into performing non-native substrate transformations. The enzyme misrecognizes these shorter carboxylic acids, termed "decoy molecules", as native substrates, thereby mistakenly initiating the catalytic cycle. As these shorter fatty acids are not hydroxylated themselves, exogenous compounds are oxidized in their stead [57,59].

The oxidation mechanisms employed by peroxidases (such as HRP [42]), peroxygenases (such as UPO) [53,54,56,77] and cytochrome P450s (such as CYP152A1, $P450_{BS\beta}$) [53,57,59,69,78] have all been well established in the literature. The formation of the highly reactive ferryl species is very similar for all three classes of enzymes mentioned, which proceeds through binding of hydrogen peroxide to the ferric enzyme, followed by heterolytic cleavage of the O-O bond, mediated by an amino acid residue acting as an acid-base catalyst. However, the oxidation of substrates via a peroxidase (or oxidase, *vide infra*) mechanism proceeds through electron transfer, whereas peroxygenase (or oxygenase, *vide infra*) proceeds via an O-atom transfer. The sequential oxidation of substrates by UPO enzymes proceeds via pathways comparable to the well described pathways of cytochrome P450 enzymes [56,69,79]. Functionalization of substrate (shown in Scheme 1 using pyrrole as an example) can occur via three different pathways [69]: i) electrophilic attack of substrate by Compound I [$(Por^{\bullet+})Fe^{IV}$=O AA], resulting in the formation of ferryl-radical substrate species that leads to a substrate epoxide intermediate; ii) H-atom abstraction by Compound I, followed by oxygen radical rebound of a caged ferryl (Compound II, [$(Por)Fe^{IV}$=O AA] or [$(Por)Fe^{IV}$-OH AA]) and substrate radical species; and iii) single electron transfer (SET) from Compound I to the substrate, followed by an electrophilic attack to the ferryl center, resulting in a ferric-cationic substrate intermediate [69]. Subsequently, further rearrangement (e.g., NIH shift, indicated by the green hydrogen atoms) leads to product formation.

As mentioned above, the proximal ligand is important for reactivity, and in the case of UPOs and CYP450, the proximal cysteine has been shown to affect the formation and stabilization of both Compound I and Compound II [69]. The one-electron reduction potential of Compound I and the pK_a of Compound II (in its protonated state, [$(Por)Fe^{IV}$-OH]) are the two physical parameters that dictate the driving force of hydrogen atom transfer (HAT) in C–H activation reactions, which can be calculated using the thermodynamic square scheme developed by Bordwell (Scheme 1, pathway ii) [69,80–82]. The pK_a of Compound II can be used to estimate the reduction potential of Compound I, which has proven difficult to determine due to its short lifetime. The difference in the pK_a values for different heme proteins is very pronounced, where heme thiolate proteins have very basic ferryl species, for example A*ae*UPO (pK_a = 10) and CYP158 (pK_a = 12.2), compared to histidine-ligated heme proteins, myoglobin (Mb) ($pK_a \leq 2.7$) and HRP ($pK_a \leq 3.5$) [69]. A high pK_a for Compound II indicates a basic [$(Por)Fe^{IV}$-OH] species with a strong O–H bond, which in turn increases the driving force of HAT by Compound I [69]. The increased basicity for heme thiolate enzymes has been associated with the cysteine proximal ligand, which pushes electron density onto the ferryl oxygen, rendering Compound II more basic, and thus turning these enzymes into potent biocatalysts [69,79,83].

Structural characterization of ferryl species by X-ray crystallography is challenging due to reduction and/or protein damage caused by radiation. However, more recently cofactor replacement of the microbial CYP450 family enzyme CYP102A1 ($P450_{BM3}$) was reported by Stanfield and collaborators as an example of a successful model for the ferryl species. The authors report the replacement of the native iron protoporphyrin IX cofactor by oxomolybdenum mesoporphyrin IX (Mo(O)PIX). The new, non-native system showed a Mo-O_{oxo} bond distance of 1.8 Å, which is virtually identical to the reported Fe-O_{oxo} bond distance for chloroperoxidase (1.82 Å); thus, this system represents an excellent model for Compound II [$(Por)Fe^{IV}$=O AA] of the classic cytochrome P450 catalytic cycle [84].

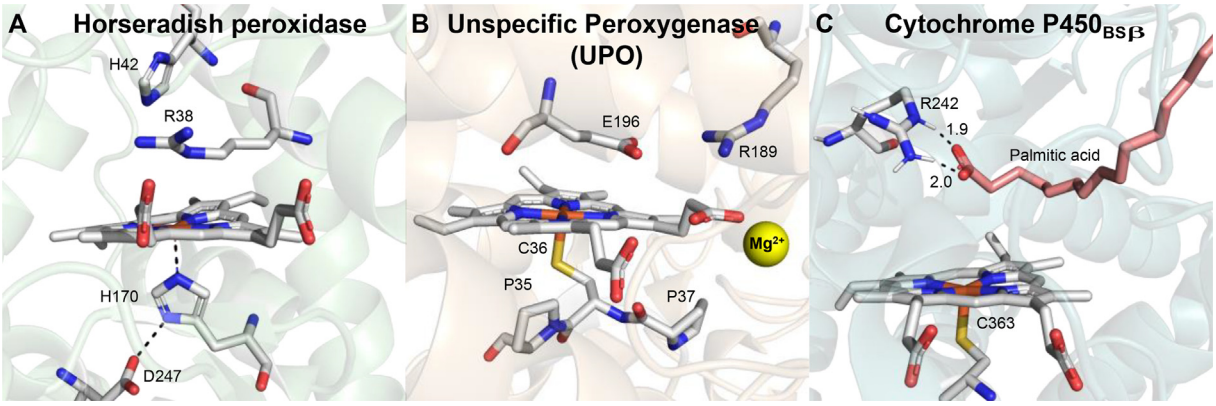

Fig. 4. Main structural differences between three classes of H_2O_2-dependent heme enzymes: A) peroxidases, represented by horseradish peroxidase, HRP (PDB: 1ATJ), B) peroxygenases, represented by mushroom *Agrocybe aegerita* (A*ae*UPO) (PDB: 2YP1), and C) bacterial cytochrome $P450_{BS\beta}$ from *Sphingomonas paucimobilis* containing palmitic acid (native substrate) (PDB: 1IZO).

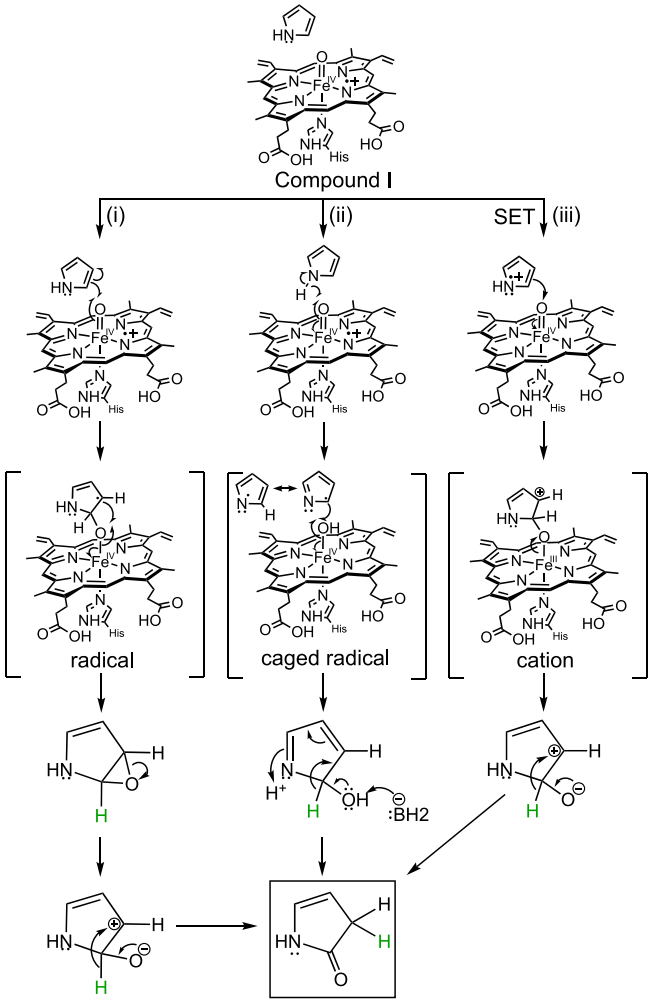

Scheme 1. Three proposed pathways for pyrrole functionalization via O-atom transfer by Compound I in heme enzymes.

2. Dehaloperoxidase peroxygenase substrates

As the number of substrates found to undergo oxygen atom transfer by DHP has dramatically increased over the past few years, the focus of this review is to provide the structural and mechanistic underpinnings of the DHP peroxygenase activity by drawing on some of the recently published results for the oxidation of indoles [8], nitrophenols [10], pyrroles [11] and cresols [7]. Literature reports on the oxidation of these substrates (and their derivatives) by other heme enzymes will be used to correlate the structure–function relationships relevant to dehaloperoxidase. For completeness, the oxidase and oxygenase functions of DHP will be introduced and briefly discussed here. In addition, electronic and structural effects are addressed and discussed in order to broaden our understanding of the function switch present in this multifunctional catalytic globin. And lastly, final remarks provide perspective on how the studies performed on DHP over the past two decades advance our understanding of catalytic globins within the context of the structure–function paradigm(s) of the heme protein superfamily.

2.1. Indole and derivatives

Dehaloperoxidase has been investigated as a biocatalyst in the oxidation of indole and derivatives in the presence of hydrogen peroxide at physiological pH by Barrios and coworkers [8]. Enzymatic assays were performed and analyzed via HPLC, with substrate conversion ranging between 24 and 48% (unoptimized) after a five-minute reaction period. Product identification by HPLC when 5-Br-indole (5-Br-I) was employed as the substrate showed 5-Br-2-oxindole and 5-Br-3-oxindolenine as the two major products formed in a 1:1 ratio. Minor products were identified as 5-Br-2,3-dioxindole, 5-Br-3-hydroxy-2-oxindole, *N*-(4-Br-2-formylphenyl)formamide, and (*E*)-5,5′-dibromo-[2,2′-biindolinylidene]-3,3′-dione (Scheme 2). The latter exhibited an intense visible band at 600 nm, which was associated with the dimer 5,5′-Br_2-indigo upon further spectroscopic investigation (oxidase mechanism, *vide infra*) [8].

Molecular dynamics (MD) simulations were originally employed to generate a geometry optimized structure, revealing 5-Br-I to be situated in the distal pocket of DHP, nearly perpendicular to the heme cofactor, with the indole nitrogen facing away from the iron center and the bromine located in the Xe1 binding site [8]. More recently, the structure of dehaloperoxidase in the presence of 5-Br-I (Fig. 5**A**) was resolved by serial femtosecond X-ray crystallography (SFX) [49]. This new structure corroborates the earlier calculated model, wherein the substrate was found to reside within the distal pocket with the halogen atom positioned internally in the Xe1 hydrophobic binding pocket. The occupancy of the Xe1 site by a substrate halogen has been previously observed for halophenols [26,47,85], haloguaiacols [6] and halocresols [7]. The amino acid F60 is displaced to accommodate the bulky halogen atom, F21 is oriented

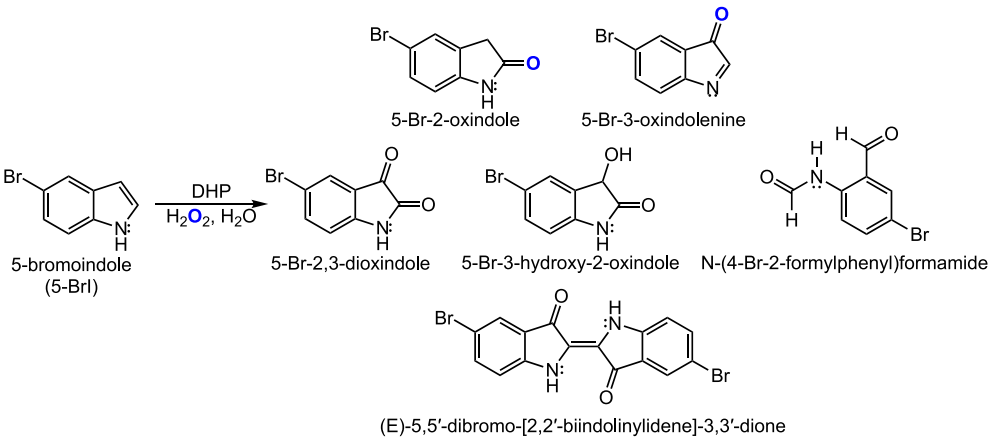

Scheme 2. Products identified in the H_2O_2-dependent oxidation of 5-Br-indole as catalyzed by DHP.

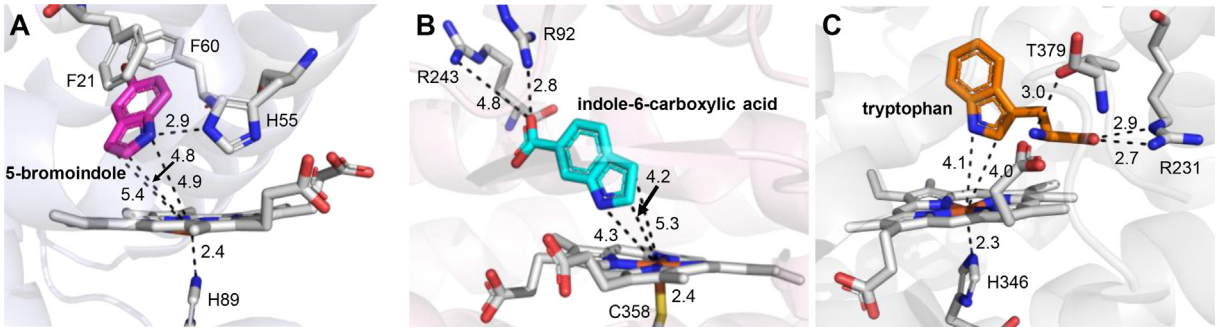

Fig. 5. Crystal structures of A) dehaloperoxidase B in the presence of 5-bromoindole (PDB: 6I6G, magenta), B) bacterial CYP199A4 complexed with indole-6-carboxylic acid (PDB: 4EGO, cyan), and C) human indoleamine 2,3-oxygenase with tryptophan (PDB: 6E46, orange). Select atomic distances (Å) and interactions between substrate and amino acids and the heme macrocycle are shown.

to form π - π interactions with the aromatic ring of the substrate, and the distal histidine (H55) is in the closed conformation interacting with the substrate via hydrogen bonding. The indole nitrogen, C2 and C3 are 4.9, 4.8 and 5.4 Å away from the heme iron center, respectively, which contributes to understanding the selective oxidation of 5-Br-I at the C2 and C3 positions [8]. The presence of the substrate inside the pocket was also confirmed by resonance Raman experiments: an increase in the 5-coordinate high spin (5cHS) heme population (and corresponding decrease of the 6cHS population) were noted upon addition of 5-Br-I to wild-type DHP. Originally, this was interpreted to be consistent with the displacement of a heme iron-bound water, as it was believed that the presence of the large 5-Br-I substrate would force the distal histidine (H55) into an open conformation [8], rendering it unable to stabilize the bound water through hydrogen bonding. However, the newly obtained SFX structure suggests that the increase in 5cHS heme instead occurs due to hydrogen bonding of the distal histidine in the closed conformation that shifts to stabilizing the substrate, rather than the iron-bound water [49].

The reactivity of indole has been reported for non-heme iron enzymes, UPOs, and cytochrome P450s (wild type and mutants, human and microbial), where the observed products were also 2-oxindole, 3-oxindole and indigo [86–94]. Bell et al. reported the catalytic activity and crystal structure of bacterial cytochrome CYP199A4 in the presence of aromatic carboxylic acids, including indole-6-carboxylic acid (Fig. 5B) [95]. The position of this substrate in the active site of the enzyme provides an explanation for the oxidation at the 2-position of the ring, because, although the authors did not observe a product by GC–MS analysis, previously published results for this substrate showed the formation of 2-indolinone-6-carboxylic acid [95,96]. Even though the positioning of indole-6-carboxylic acid in the CYP199A4 structure differs from what was found for 5-Br-I in DHP [49], the distances between the heme-Fe and the indole nitrogen, C2 and C3 atoms (4.3, 4.2 and 5.3 Å, respectively) are comparable to those found for DHP. Additionally, a recently published crystal structure of human indoleamine 2,3-dioxygenase 1 (IDO1) complexed with its native substrate tryptophan (Fig. 5**C**), reveals an orientation that favors oxidation at the C2 position, (distances from indole nitrogen and C2 to the heme-Fe are 4.1 and 4.0 Å, respectively) [97,98], similar to what has been observed for indolic substrates bound to DHP and CYP199A4.

In the DHP-catalyzed oxidation of 5-Br-I, isotopically labeled water and hydrogen peroxide ($H_2^{18}O$ and $H_2^{18}O_2$) indicated that the source of the oxygen incorporated into the substrate was derived from hydrogen peroxide, providing unequivocal evidence that the substrate was oxidized via a peroxygenase mechanism. These results, in conjunction with stopped-flow UV–visible spectroscopic data, allowed for the proposal of a mechanism for the H_2O_2-dependent oxidation of haloindoles by DHP [8]. While it focused on the observed heme intermediate species and not on a step-by-step substrate-based mechanism, the authors mention the possibility of oxygen rebound chemistry or other mechanisms associated with peroxygenase/CYP450 enzymes, such as i) H-atom abstraction yielding a caged substrate radical and ferryl intermediate, ii) electrophilic addition followed by formation of an epoxide intermediate or iii) SET followed by electrophilic attack (Scheme 1 and Fig. 6).

Previous mechanistic reports of the oxidation of indole by the heme enzyme IDO1 suggest that the formation of the products 2-oxindole and 3-oxindole products is likely to proceed via an epoxide intermediate or by hydroxylation [88,94,99], similar to cytochrome P450 catalyzed reactions. The report made by Barrios et al. corroborates the assumption about the possible mechanistic pathways for the DHP-catalyzed oxidation of indole derivatives [8].

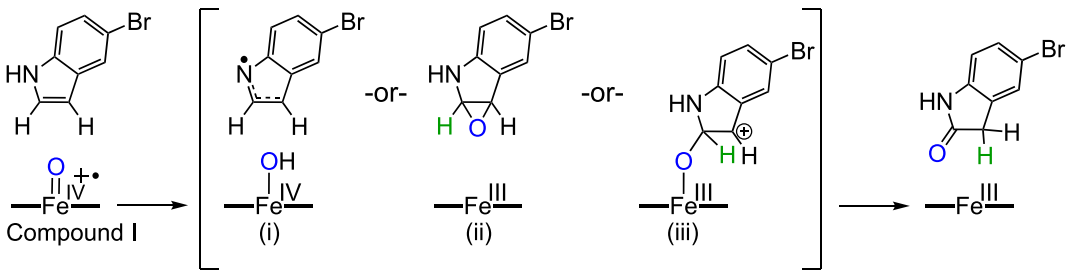

Fig. 6. Possible intermediates for the H_2O_2-dependent oxidation of 5-bromoindole to 5-bromo-2-oxindole: (i) caged substrate radical and ferryl species intermediate, (ii) epoxide intermediate, and (iii) ferric–cationic substrate species. The green hydrogen atom represents a label that would undergo an NIH shift in the cases of ii and iii [69]. Note: for simplicity, the 5-bromo-3-oxindole product that was also formed in a ~ 1:1 ratio, is not shown but is proposed to involve the same intermediates as depicted above for 5-bromo-2-oxindole.

2.2. Pyrrole and derivatives

Un- or lightly-substituted pyrroles are heterocyclic aromatic compounds that are highly unstable in the presence of light, acid and oxygen conditions. The rapid, spontaneous formation of polypyrrole often hinders the use of this chemical as a scaffold for sequential chemical reactions [100,101]. Thus, the synthesis of substituted pyrroles can be costly, laborious and environmentally unfriendly [100].

Enzyme catalyzed pyrrole oxidation to polypyrrole has been reported for HRP and laccase due to the technological application of this product as a conducting polymer [102,103]. Guengerich et al. also reported the use of oxygenases, such as CYP450, in the activation and catalysis of pyrrole, although the authors do not mention the nature of the product(s) formed [101].

McCombs et.al. employed the multifunctional globin DHP as a biocatalyst for the functionalization of pyrroles under physiological conditions [11], where 32% conversion (unoptimized) of pyrrole to 4-pyrrolin-2-one and 3-pyrrolin-2-one in a 1:9 ratio was achieved after 5 min of reaction (Scheme 3). Methylated pyrrole derivatives were also investigated (*N*-methyl, 2-methyl, 3-methyl and 2,5-dimethylpyrrole) and exhibited increased conversion compared to the parent compound. Substituted pyrroles showed the formation of multiple monomeric products, with the 2-one being the major product. Trace oligomeric products were observed at longer reaction times (24 h) by LC-MS. The functionalization of pyrroles at the α -position was expected and electrophilic attack at this position has been found to be kinetically favored owing to the large orbital coefficients in the HOMO for C2 and C5 and the higher stability of the σ-complex intermediate formed in the oxidation of these compounds [104].

The single oxygen atom incorporated at the α -position of the ring was confirmed by ^{18}O labeling studies to have originated from a hydrogen peroxide molecule, providing strong evidence of oxidation by a peroxygenase mechanism [11]. Mechanistic studies performed by stopped-flow UV–visible and rapid-freeze-quench electron paramagnetic resonance (RFQ-EPR) spectroscopies allowed for the proposal of a stepwise catalytic cycle for the H_2O_2-dependent oxidation of pyrrole: a single, two-electron electrophilic addition of the ferryl oxygen of Compound I to pyrrole forms a cationic tetrahedral-like intermediate complex, which undergoes further rearrangement forming the 4-pyrrolin-2-one product [11]. The authors propose that the distal histidine (H55) is likely acting as the acid/base, and further rule out the possibility of a mechanism involving radicals due to the absence of polypyrrole formation, which is initiated by the coupling of two pyrrole radical cations [11]. Pyrroles are more likely to undergo electrophilic attack owing to their electron rich nature [104], and a cationic intermediate has been established to be common when the product formed is a ketone or an aldehyde [69]. This cationic intermediate, described in the mechanism proposed by McCombs et al. in one simplified step, may also be formed from two discrete, one-electron steps, where a single electron transfer (SET) from Compound I to substrate is followed by electrophilic attack of the ferryl oxygen to the activated substrate (Scheme 2, Pathway iii) [69].

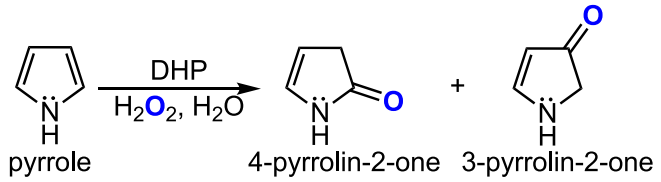

Scheme 3. Products identified in the H_2O_2-dependent oxidation of pyrrole as catalyzed by DHP.

2.3. Nitrophenol and derivatives

In addition to its ability to degrade naturally occurring phenolic compounds, DHP also possesses the ability to oxidize metabolites of anthropogenic origins. The U.S. Environmental Protection Agency (EPA) lists 2-nitrophenol (2-NP), 4-nitrophenol (4-NP), 2,4-dinitrophenol (2,4-DNP) and 2,4,6-trinitrophenol (2,4,6-TNP) as Priority Pollutants [105], the majority of which were also found to be substrates (except 2,4,6-TNP) for DHP that are oxidized via a peroxygenase mechanism [10].

The enzymatic assays analyzed via HPLC were performed in the presence of ferric WT DHP, hydrogen peroxide and the aforementioned substrates at pH 6, and showed a conversion range of 16–50% after five minutes (unoptimized). In the case of 4-nitrophenol, three main products were identified: 4-nitrocatechol (4-NC), which was further oxidized into 5-nitrobenzene-triol (two isomers possible), and even further to form hydroxy-5-nitro-1,2-benzoquinone (Scheme 4). In order to determine the origin of the oxygen atom inserted in the substrate, ^{18}O-labeling studies ($H_2^{18}O$ and $H_2^{18}O_2$) were performed, revealing that the oxygen incorporated into 4-NP yielding 4-NC is derived from a H_2O_2 molecule, consistent with a peroxygenase mechanism [10]. Interestingly, however, the labeling studies also demonstrated that the other oxidation products were formed through successive peroxidase-based oxidations. Three sequential oxidations by two different mechanisms (peroxygenase-peroxidase-peroxidase) yielding the hydroxy-5-nitro-1,2-benzoquinone product demonstrates the nature of DHP as a multifunctional catalyst (Scheme 4).

The enzymatic ortho-hydroxylation of 4-NP has been reported for both fungal UPOs [67] and mammalian CYP450 enzymes (CYP2E1 and CYP3A4) [106–109]. The substrate was established to be an *in vitro* probe to the O_2/NADPH-dependent catalytic activity for the P450 family of enzymes and chromatographic [106] and spectrophotometric [109] methods have been developed to detect the formation of the *o*-catechol product. Additionally, Raner et al. reported the oxidation of 4-NP (to 4-NC) and 4-NC (yielding 2,3,4-trihydroxonitrobenzene) using Cytochrome $P450_{BM3}$ [110,111]. The reaction of 4-NP and 4-NC by $P450_{BM3}$ requires NADPH and molecular oxygen, and the authors proposed that the

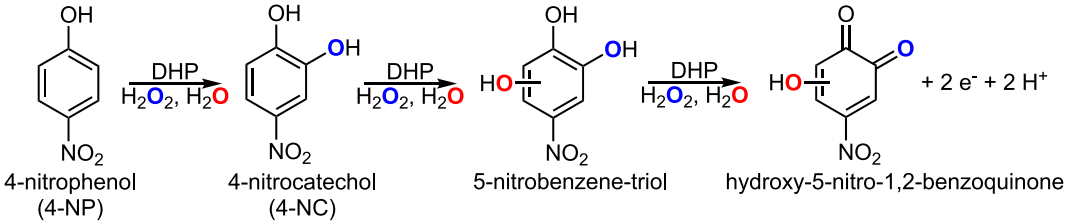

Scheme 4. Products identified in the H_2O_2-dependent oxidation of 4-nitrophenol as catalyzed by DHP.

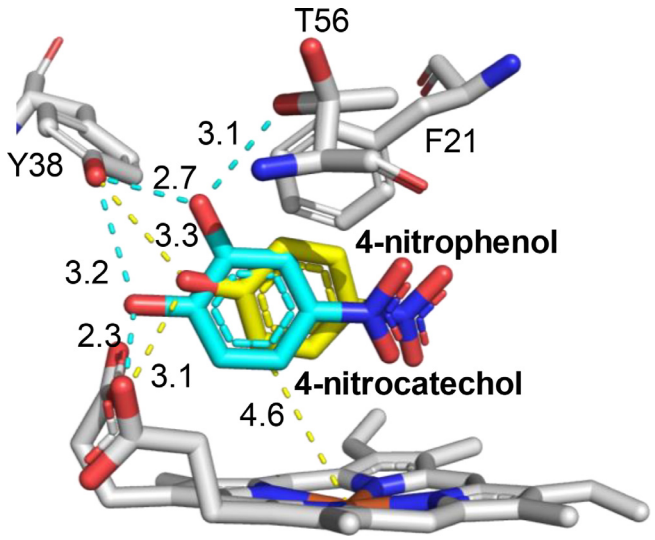

Fig. 7. Crystal structures of dehaloperoxidase complexed with 4-nitrophenol (PDB: 5CHQ, yellow) and the oxidation product 4-nitrocatechol (PDB: 5CHR, cyan). Select atomic distances (Å) and interactions between the substrate (color coordinated) and active site amino acids or the heme macrocycle are shown.

mechanism occurs via the formation of an epoxide intermediate, a more common pathway for the hydroxylation of the aromatic substrates [110]. Thus, whilst DHP and $P450_{BM3}$ are both capable of oxidizing 4-NP to trihydroxynitrobenzene, DHP accomplishes this via two different activities (peroxygenase and peroxidase), whereas $P450_{BM3}$ performs two successive monooxygenations.

McCombs et al. were also able to obtain X-ray crystal structures of both 4-NP and 4-NC complexes with dehaloperoxidase (the first reported structures of a heme protein in complex with these compounds), which show the substrate and product are in the distal pocket and oriented perpendicular to the heme plane (Fig. 7). The *o*-CH of the substrate and the heme iron are in close proximity (~4.6 Å), and taking into account that the bond length of Fe-O in the active species Fe(IV)=O is around 1.8 Å [69], hydroxylation at the ortho-position of the ring was expected. The hydroxyl group of both 4-NP and 4-NC is pointed towards the γ heme edge, and the nitro groups are positioned internally. Hydrogen bonding interactions with Y38, T56 and the heme propionates, as well as π - π stacking interactions with F21, provide additional stabilization. The rotation of the product to position the *o*-OH group towards hydrophilic amino acids such as Y38 and T56 was expected seeing that the product is more polar than the parent compound [10].

Similar to the oxidation mechanism of haloindoles by DHP [8], the peroxygenase mechanism proposed for the oxidation of 4-nitrophenol to 4-nitrocatechol focused on the heme intermediate species and not on the stepwise mechanism of substrate oxidation. In addition, the authors do not propose a mechanism for the sequential peroxidase mechanisms taking place after the formation of 4-NC. However, the authors mention that the oxidation of the substrate most likely occurs through an oxygen radical rebound mechanism, but they do not rule out the possibility of O-atom incorporation by another mechanism (Fig. 8) [10].

2.4. Cresol and derivatives

Methylphenols, commonly known as cresols, are released into the environment from industrial waste, such as the combustion of petroleum and wood. Due to their environmental toxicity and persistence, these chemicals were included in the Environmental Protection Agency (EPA) Priority Pollutants List and Toxic Substances Control Act [105,112].

The reactivity of cresols with DHP in the presence of H_2O_2 was demonstrated by HPLC and the studied substrates displayed a range of 32–68% conversion after five minutes of reaction (unoptimized). Product identification showed two distinct monomeric products for select substrates, the 2-methyl-1,4-benzoquinone and the *o*-catechol derivatives [7]. It is also worth mentioning that oligomeric products (n up to 6) were also identified, which could be the result of subsequent quinone radical coupling reactions. Labeling studies using enriched $H_2^{18}O$ and $H_2^{18}O_2$, performed on 4-bromo-*o*-cresol (4-Br-C) as a representative substrate, showed that the formation of 2-methyl-1,4-benzoquinone occurred via a peroxidase mechanism, where the source of the oxygen was a water molecule. The oxygen inserted at the ortho-position of 4-Br-C to generate 5-bromo-3-methyl-1,2-benzediol (an *o*-catechol derivative) originated from a hydrogen peroxide molecule, consistent with a peroxygenase mechanism (Scheme 5). The same oxyfunctionalization pattern was also observed for other cresols: 4-X-*o*-cresol (X = H, F, Cl, Br, NO_2) and 4-X-*m*-cresol (X = H and Cl), whereas 4-Me-*o*-cresol and *p*-cresol only yielded the *o*-catechol derivative 3-methyl-1,2-benzediol. Dehaloperoxidase is therefore employing both peroxidase and peroxygenase mechanisms in the oxidation of cresols in a non-preferential manner, a result that had not been previously observed for this enzyme [7].

Structural studies performed using X-ray crystallography revealed that the cresol substrates bind in the hydrophobic distal pocket of DHP in different positions (Fig. 9). The structure of 4-bromo-*o*-cresol (4-Br-C) and *p*-cresol showed both substrates in the hydrophobic binding pocket, the former buried inside and the latter closer to the entrance of the pocket (γ edge). The halogen atom of 4-Br-C is located in the Xe1 binding cavity displacing the residue F60, similar to the 5-Br-I structure (Fig. 4**A**), while the hydroxyl group is found pointing towards the iron center and interacting with H55 in the closed conformation. On the other hand, *p*-cresol is perpendicular to the heme cofactor, and the hydroxyl group of *p*-cresol is interacting with the propionate group D, Y38 and T56. To accommodate *p*-cresol, H55 is in the open conformation [7].

The biodegradation of cresols has been reported for other enzymes, such as UPO (peroxygenase) [67], HRP and CPO

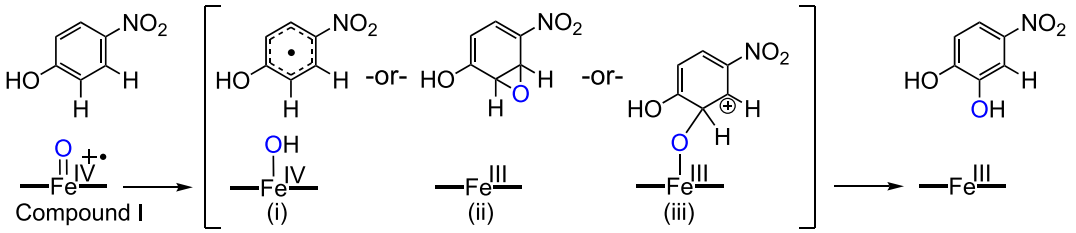

Fig. 8. Possible intermediates for the H_2O_2-dependent oxidation of 4-nitrophenol to 4-nitrocatechol (i) caged substrate radical and ferryl species intermediate, (ii) epoxide intermediate, and (iii) ferric–cationic substrate species.

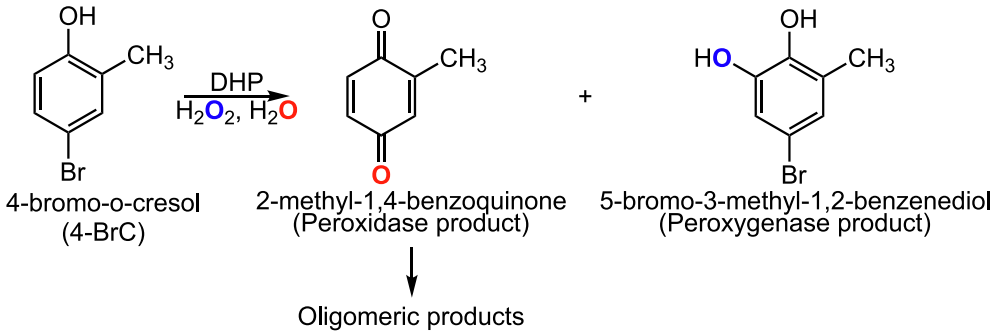

Scheme 5. Products identified in the H_2O_2-dependent oxidation of 4-bromo-*o*-cresol as catalyzed by DHP.

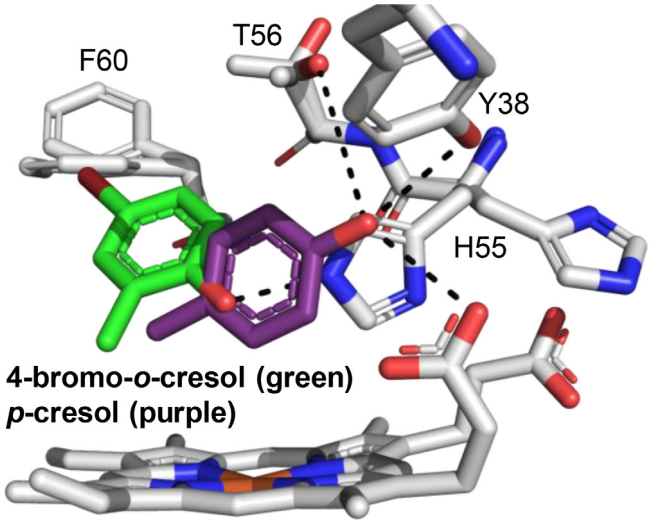

Fig. 9. Crystal structures of dehaloperoxidase complexed with 4-bromo-*o*-cresol (PDB: 6ONX, green) and *p*-cresol (PDB: 6OO6, purple). Select atomic distances (Å) and interactions between substrate, amino acids and the heme macrocycle are shown.

(peroxidase) [67,113] as well as for microorganisms, such as bacteria and fungi. However, to the best of our knowledge, the study by Malewschik et al. is the only report on the reactivity of cresols that includes mechanistic, spectroscopic and structural studies [7]. Mechanisms for each of the DHP-catalyzed activities employed in the oxidation of cresols were proposed: a peroxidase-based one that accounts for the formation of the 1,4-benzoquinone product, and a peroxygenase-based one that leads to the formation of the *o*-catechol product. The latter was in accordance with the most recent mechanism proposed for the DHP-catalyzed oxidation of pyrroles [11], and also in agreement with well-known cytochrome P450 pathways [69]. The authors proposed two different pathways for the formation of the catechol derivative, electrophilic attack of the substrate with Compound I or oxygen rebound, but no further investigations were mentioned to determine a definitive pathway (Fig. 10).

The oxidation of cresols and derivatives has expanded the number of phenolic compounds in the EPA Priority Pollutants list which can be oxidized by DHP to 10 out of 11 [7], and suggests that this catalytic globin may be promising in applications as a bioremediation catalyst, as previously posited by Lebioda and coworkers [5].

3. O_2-Dependent DHP activities

3.1. Oxidase activity

Oxidase enzymes are ubiquitous in nature, and are responsible for the oxidation small molecules [114–116], electron transport [117–120] and formation of reactive oxygen species [121,122]. They possess a variety of different cofactors, including heme and non-heme iron, multi-copper centers, and flavin. The cofactors mediate redox processes in the presence of molecular oxygen as the oxidizing agent, and when oxidative dehydrogenation occurs (hydrogen atom abstraction), it leads to the formation of H_2O or H_2O_2 [123].

The catalytic globin DHP was found to possess an oxidase activity, discovered in 2014 during the investigation of the peroxygenase activity with 5-bromoindole (5-Br-I) as a representative substrate. The reaction led to the formation of two major products, 5-Br-2-oxindole and 5-Br-3-oxindolenine and one minor product of interest (*E*)-5,5′-dibromo-[2,2′-biindolinylidene]-3,3′-dione (substituted indigo). Labeling studies with $^{18}O_2$, non-enzymatic and non-oxidant controls were performed, indicating that the formation of both 3-oxindolenine and the substituted indigo were dependent on both DHP and O_2 [8].

The reaction of 5-Br-3-oxidole with DHP in the presence of O_2 yielded 5-Br-3-oxindolenine (Fig. 11, top). In addition, the formation of the indigo product, first identified by HPLC, was further assessed by UV–visible spectroscopy. The reductant, 5-Br-3-oxindole (λ_{max} = 383 nm), was generated *in situ* using

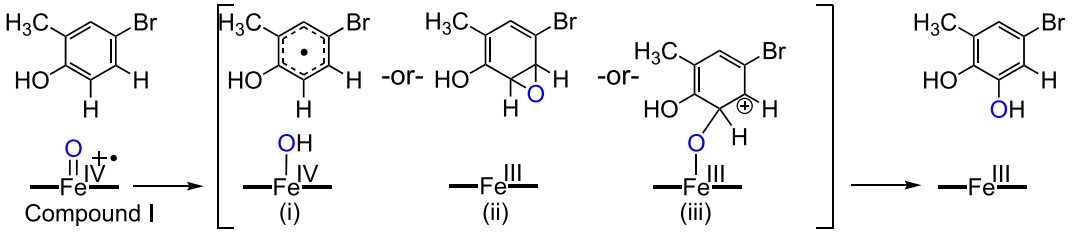

Fig. 10. Possible intermediates for the H_2O_2-dependent oxidation of 4-bromo-*o*-cresol to the *o*-catechol product (i) caged substrate radical and ferryl species intermediate, (ii) epoxide intermediate, and (iii) ferric–cationic substrate species.

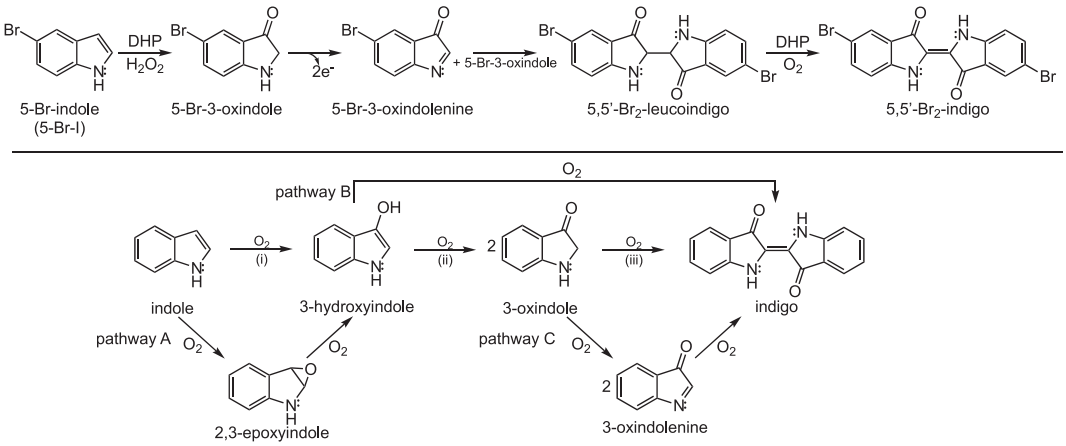

Fig. 11. Top) Oxidase activity performed by DHP in the presence of O_2 where the *in situ* generated 5-Br-3-oxindole forms 5-Br-3-oxindolenine, which ultimately leads to the formation of 5,5′-Br_2-indigo. Bottom) Different pathways (pathway A-C) for the formation of indigo catalyzed by oxygenase and oxidase enzymes: A) 2,3-epoxyindole intermediate in the formation of the 3-hydroxyindole product, B) oxidation of the 3-hydroxyindole product to form indigo, C) formation of two intermediates, 3-oxindole and 3-oxindolenine.

5-Br-3-acetoxyindole (25 equiv.) and liver esterase, in the presence of DHP under aerobic conditions, which led to the formation of 5,5′-Br_2-leucoindigo as an intermediate, before the formation of 5,5′-Br_2-indigo (λ_{max} = 289 and 640 nm) [8].

Indigo has been observed previously in the oxidation of indole when catalyzed by cytochrome P450s, UPOs, and indoleamine 2,3-dioxygenase (Fig. 11, bottom). The first step is the hydroxylation of indole at the C3 position, performed by oxygenase enzymes (*vide infra*) [94], either by direct hydroxylation of the substrate (CYP450) (Fig. 11, bottom, step i), or by formation of an epoxide intermediate (UPOs) (Fig. 11, bottom, pathway A) [94]. The 3-hydroxyindole product is then further oxidized to form indigo (Fig. 11, bottom, pathway B) [94,124]. In addition, the 3-hydroxyindole can be oxidized to form 3-oxindole (Fig. 11, bottom, step ii) [99], where two equivalents of this product can lead to the formation of indigo directly (Fig. 11, bottom, step iii), or undergo further oxidation to form an intermediate product 3-oxindolenine, observed in the IDO1 oxidation pathway (Fig. 11, bottom, pathway C) [99]. The enzyme HRP has also been found to catalyze the oxidation of indoles to form indigo, which was proposed to proceed via a hydroperoxide intermediate. After water elimination, 3-oxindolenine was formed, which is further oxidized to form a 3-oxindole radical that undergoes radical coupling to form the final product (not shown) [125].

3.2. Oxygenase activity

Oxygenases are a class of enzymes, which use molecular oxygen for substrate functionalization. They can be subdivided into monooxygenases or dioxygenases (insertion of one or two oxygen atoms, respectively) [126]. These enzymes have been found to catalyze the oxidation of a variety of different substrates, such as phenols [127], catechols [128], amino acids and proteins [98,129], lipids and fatty acids [129,130], amongst others. Similar to oxidases, oxygenases possess different cofactors, such as heme and non-heme iron, mono and multicopper centers, manganese, and flavins [123,126,131–134].

Dehaloperoxidase has been found to exhibit oxygenase activity in the oxidation of 2,3-dimethylindole (McCombs, Ph.D. dissertation 2017) [9]. The major products identified were 3-hydroxy-2,3-dimethylindole (3H-DMI) and *o*-acetamidoacetophenone (*o*-AAP). Minor products were identified to be 2-carboxyaldehyde-2-methylindole and 3-carboxy-2-methylindole (Scheme 6). The origin of the oxygen atom(s) inserted into the major products was determined by isotopic labeling studies employing $^{18}O_2$, which indicated that the O-atom(s) were derived from molecular oxygen. The formation of the major products, 3H-DMI and *o*-AAP, could have originated from monooxygenase and dioxygenase activities, respectively. Alternatively, the *o*-AAP product could have been formed by two sequential monooxygenase steps. Further studies need to be performed to differentiate between these two possibilities [9].

Examples of enzymes that perform monooxygenation reactions are cytochrome P450 enzymes, lipoxygenase, and naphthalene 2,3-dioxygenase, among others. The cytochrome P450 family of enzymes has been found to hydroxylate indole at the C3 position as an intermediate for the formation of indigo (Fig. 11**B**, step i) [94]. Lipoxygenase inserts O_2 into polyunsaturated fatty acids

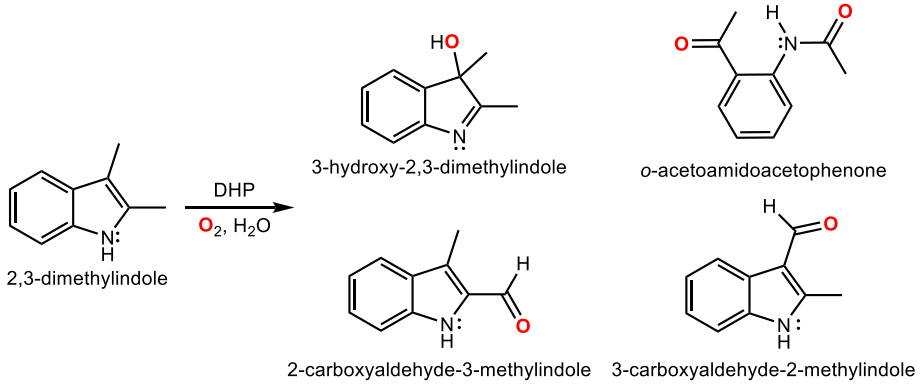

Scheme 6. Products identified in the O_2-dependent oxidation of 2,3-dimethylindole as catalyzed by DHP.

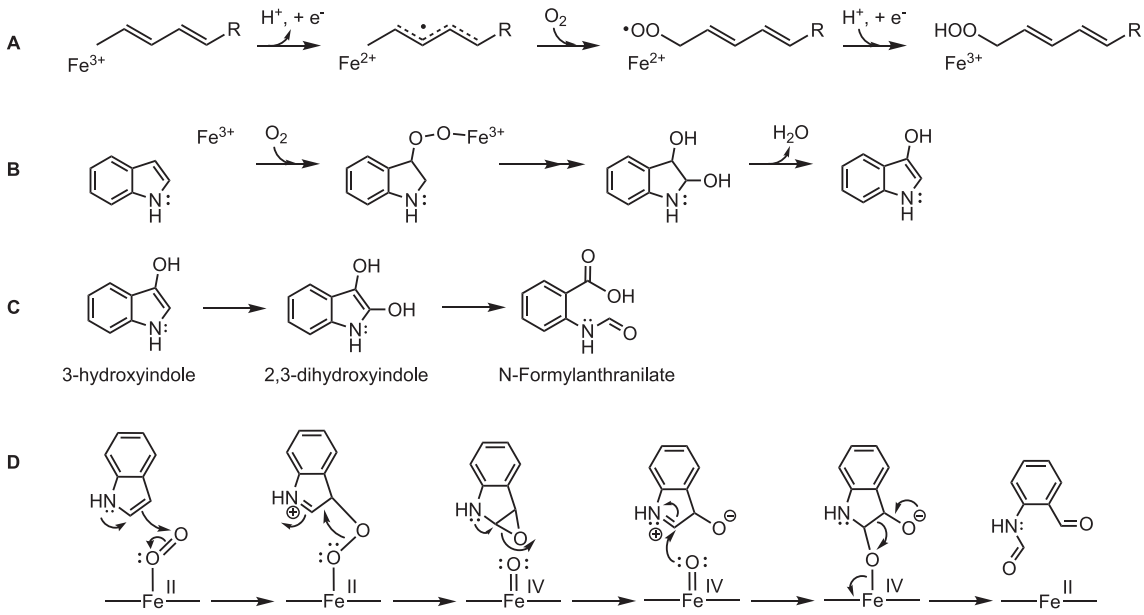

Fig. 12. Oxygen insertion catalyzed by mono- and dioxygenase enzymes A) hydroperoxo functionalization of polyunsaturated fatty acids catalyzed by lipoxygenase, B) hydroxylation of indole catalyzed by naphthalene 1,2-dioxygenase (NDO), C) hydroxylation and ring cleavage of indole observed for microbial organisms, and D) ring cleavage of indole catalyzed by tryptophan dioxygenases.

and the final product possesses a hydroperoxo moiety, which can undergo sequential oxidation, reduction rearrangement, and/or lysis to afford smaller products (Fig. 12, pathway A) [130,135]. Naphthalene 1,2-dioxygenase (NDO) performs the hydroxylation of aromatic molecules, such as indole (Fig. 12, pathway B). The indole-O-O-Fe adduct is an intermediate complex, leading to the formation of the 3-hydroxyindole product after water elimination from indoline-2,3-diol [136]. UPOs have also been found to catalyze the formation of 3-hydroxyindole, however the intermediate was observed to be 2,3-epoxyindole [94]. The final product of both the NDO- and UPO-catalyzed oxidation of indole is indigo [94].

Ring opening products from indole (kynuric products) have been observed in microbial biotransformations, where sequential hydroxylation of the substrate has been reported, followed by cleavage of the pyrrole ring to yield the *N*-formylanthranilate product (Fig. 12, pathway C). This product can undergo further oxidation and the smaller products are used as carbon, nitrogen and oxygen sources for these organisms [124]. HRP, a canonical peroxidase enzyme, has been reported to oxidize a series of substituted indoles into their respective kynuric products in the presence of O_2 and H_2O_2, proposed to occur via a dioxetane intermediate (not shown) [125]. Additionally, tryptophan 2,3-dioxygenase and IDO1 are enzymes that perform the insertion of two oxygen atoms into their respective substrates, followed by pyrrole ring cleavage. The mechanism of oxygenation is thought to proceed via the formation of a substrate cation (Fig. 12, pathway D) or radical, which leads to either an epoxide or dioxetane intermediate [98,137].

McCombs and coworkers suggest that the oxidation of 2,3-dimethylindole by dehaloperoxidase is following an O_2-dependent radical-based mechanism similar to the lipoxygenase pathway [9]. In addition to $^{18}O_2$ labeling studies, the following were observed: i) in the absence of an oxidant and under anaerobic conditions no reactivity was observed, ii) the presence of radical scavengers in solution was shown to hinder the reactivity of the enzyme with the substrate, which suggests a radical-based mechanism and iii) anaerobic studies performed in the presence of ferric DHP, 2,3-DMI and carbon monoxide shows the formation of an Fe^{II}-CO adduct, indicating that the substrate reduces the enzyme to a ferrous state, a result that was also confirmed by resonance Raman studies. Overall, the authors do not propose a stepwise mechanism for the formation of the main products, 3H-DMI and *o*-AAP, but suggest that the indole hydroperoxide as the primary intermediate, similar to the lipoxygenase product (Fig. 12, pathway A) [9].

4. Electronic and structural effects: How DHP differentiates between activities

4.1. Redox properties

Dehaloperoxidase possesses an unusually high redox potential for the Fe(III)/Fe(II) couple for both DHP A and DHP B (+204 and + 206 mV vs. SHE respectively) [17,138] compared to other heme proteins, such as HRP (E° = −270 mV [139]), cytochrome P450 (E° = −270 mV [140]), and other globins (Mb = +59 mV [141] and, Hb = +158 mV [142]). Additionally, the Fe(IV)/Fe(III) reduction potential for DHP was estimated to be ~ 1.58 V [10,25], which is higher than that for HRP (E° = +0.92 V [140]) and UPO (E° = +0.80 V [77]). These high reduction potentials could facilitate the reactivity of DHP with the wide substrate scope (Fig. 1) and allow this multifunctional globin to perform these different oxidative activities [10,25].

As previously mentioned, the proximal side of heme enzymes plays a vital role in the formation of the active oxygen species (*vide supra*). The proximal cysteine ligand present in peroxygenases and CYP450s is an excellent electron donor, conferring these proteins with their ability to perform the oxyfunctionalization of inactivated C–H bonds. Thus, as an illustrative example, the proximal histidine of myoglobin was replaced with a cysteine via site-directed mutagenesis, which considerably decreased the E° ((Fe(III)/Fe(II)) of Mb from + 59 to − 230 mV [140]. In addition, the catalytic triad (e.g., the Asp-His-Fe in peroxidases and the PCP motif in UPOs) also plays an important role in the reactivity of these enzymes. Efforts were made in installing an Asp-His-Fe triad in DHP, where a local methionine was replaced with an aspartate residue (M86D). However, the mutant presented attenuated activity towards oxidation of 2,4,6-trichlorophenol (peroxidase activity) compared to the wild type enzyme (~4-fold decrease). Whilst the resultant changes in redox properties (+202 mV vs SHE for WT

DHP vs. + 76 mV vs. SHE for M86D) typically favor an increase in peroxidase activity, this was outweighed by the formation of a 6cLS system, where the sixth ligand was proposed to be the distal histidine or a strongly bound solvent molecule, which precluded H_2O_2-binding and led to significantly less peroxidase activity compared to the WT enzyme [52].

The presence of a substrate in the binding pocket of heme proteins has been found to alter the redox potential of the system, facilitating catalytic activity. A classic example is the catalytic cycle of cytochrome P450, where upon substrate binding, the spin state of the iron changes from low to high spin, accompanied by a positive change in the redox potential (e.g., P450 −330 mV to $P450_{cam}$ −163 mV [143]). Only then can the redox partners transfer an electron to the heme cofactor, leading to dioxygen binding and formation of a resultant Fe(III)-superoxide that further undergoes reduction and O-O bond cleavage, yielding the Compound I active species [144,145]. Thus, in addition to the contribution attributed to the protein scaffold, the redox potential of the protein can be fine-tuned by altering the environment around the heme prosthetic group. It is known that the introduction of hydrophobic or aromatic interactions into the secondary coordination sphere (SCS) of the heme as well as new hydrogen bonds between the substrate and surrounding amino acids (both the proximal and distal sides) can exert an impact on the enzyme's redox potential [140]. Additionally, the presence of a negative charge or dipoles around the metal can decrease the redox potential by stabilizing higher oxidation states, which could facilitate catalytic activity [139,140]. Lastly, the propionate groups, the "electrostatic anchors" of heme proteins, play an important role in catalysis and electron transfer processes where hydrogen bonding interactions, either from a substrate molecule or by surrounding amino acid residues, can tune the reactivity of the heme [146].

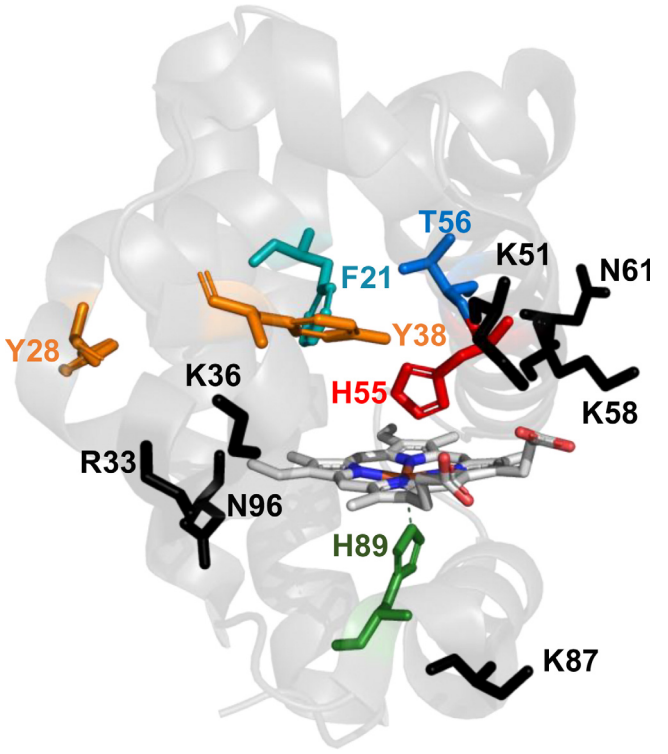

Fig. 13. Structure of DHP highlighting the amino acid residues that were targeted for site-directed mutagenesis (PDB: 6I6G). Amino acid numbering follows that for DHP B, however some of the mutagenesis studies were performed using DHP isoenzyme A [17,36,38,44].

4.2. Structural effects: Site-directed mutagenesis

Site-directed mutagenesis studies of amino acids located either within the distal cavity or on the surface of DHP have been used to evaluate the role of specific residues with respect to catalytic activity (Fig. 13):

i) Mutagenesis studies were performed on the distal histidine (H55D, H55N, H55R, H55V, Fig. 13, red) and their activities evaluated: H55D and H55N showed 6-fold and 11-fold attenuated activity, respectively, for the oxidation of 2,4,6-TCP compared to the WT enzyme. The mutant H55D could display an open/closed configuration, as shown by structural studies (~100% open conformation, solvent exposed) and FTIR (carbonmonoxy form, closed conformation), which provided an explanation for the partial peroxidase activity compared to the WT enzyme. The H55R mutant was shown to be protonated and in the open conformation, retaining only 16% of WT DHP's peroxidase activity (2,4,6-TCP/TBP), while H55V was shown to be virtually inactive. These studies highlighted the importance of the distal histidine as an acid-base catalyst [23,147].

ii) In addition, the proximal histidine was exchanged for a glycine residue (H89G, Fig. 13, green), which showed an approximate 5.6-fold and 16-fold decrease in the oxidation of 2,4,6-TCP and 2,4,6-TBP respectively [23,147], compared to WT;

iii) Mutations to T56 (Fig. 13, blue) were also studied as this residue was hypothesized to be critical to the distal histidine (H55) conformational flexibility. T56G was found to have a 5-fold lower enzymatic efficiency (k_{cat}/K_M) with respect to 2,4,6-TCP oxidation compared to the WT enzyme, a result that showed that T56 is required for maintaining the distal histidine in position for optimal peroxidase activity [20]. Even though the other mutants exhibited increased enzymatic efficiency (k_{cat}/K_M) compared to WT DHP (T56S, ~2-fold; T56A, ~3-fold; T56V, 1.3-fold), most likely attributed to lower steric hindrance which confers H55 with more flexibility, the same mutants also displayed an increased formation of a stable, hexacoordinate hemichrome species (i.e, Fe-H55 adduct) which has been implicated in enzyme inactivation [51];

iv) Compound ES, a ferryl species with a radical on a local amino acid residue [(Por)Fe^{IV}=O $^{\bullet}$AA], is the typically observable activated species in the absence of substrate. Replacement of tyrosine residues Y28 and Y38 with redox-inactive phenylalanines (Y28F/Y38F - Fig. 13, orange) led to the formation of an alternative active catalytic species, Compound I [($Por^{\bullet+}$) Fe^{IV}=O AA], a ferryl species with a porphyrin π -cation radical. Single-point mutations (Y28F or Y38F) still showed the formation of Compound ES, thus showing that either of the tyrosine residues are capable of reducing the porphyrin π -cation radical of Compound I. Even though the double-mutant Y28F/Y38F showed an increased catalytic efficiency for the oxidation of 2,4,6-TCP (~1.6-fold) compared to WT, it also suffered from an increased rate of heme bleaching. Thus, the tyrosine residues in the WT enzyme act as endogenous reductants to quench Compound I, which helps prevent irreversible oxidative damage to the protein scaffold by leftover oxidizing equivalents due to inefficient substrate oxidation and/or absence of substrate altogether [25,69,148];

v) Electrostatic effects were investigated with surface mutations (N96D, R33Q, R33A, K36A, N61D, N61K, K58A, K51A, K87A - Fig. 13, black). These studies demonstrated that mutants that led to a more negative charge on the surface of the enzyme exhibited an attenuated catalytic efficiency

in the oxidation of 2,4,6-TCP compared to WT DHP (varied from 0.6 to 0.89-fold). Conversely, the mutant N61K that introduced a more positive charge compared to WT DHP displayed an increase in enzymatic efficiency for 2,4,6-TCP oxidation (~1.2-fold). These results suggested that surface electrostatics play a central role in the catalytic activity, and is likely affecting substrate binding given the pK_a of 6.2 for 2,4,6-TCP [149];

vi) The F21W mutant (Fig. 13, cyan), wherein phenylalanine within the distal cavity of DHP was substituted by tryptophan, was found to decrease peroxidase activity in the oxidation of 2,4,6-TCP (>7-fold decrease) while showing virtually no change in peroxygenase function in the oxidation of haloindoles (1.2–2.1-fold decrease). Previous structural studies show that TCP has two distinct binding sites in the DHP distal cavity [26], which in turn represent two different functions: TCP_{ext} is a solvent exposed position and inhibits peroxidase function, and TCP_{int} is buried in the pocket where it undergoes oxidation (Fig. 14**A**). The F21W mutant places a large amino acid residue where the TCP_{int} binding site is, thus the peroxidase activity is decreased due to steric hindrance, whereas TCP_{ext} remains viable for binding peroxygenase substrates. These results show that selective tuning of DHP activity can be accomplished via single point mutations, without affecting H_2O_2 activation despite H55 being in the open conformation [26,150].

Most of the aforementioned mutagenesis studies focused on the peroxidase function of DHP, given that the other native functions of DHP were not identified until more recently. However, the results highlighted that the majority of structural modifications of the protein's amino acid sequence have a negative effect on catalytic activity, and that positive effects are accompanied by changes that lead to protein inactivation. Overall, these studies indicate that the native protein structure of DHP is robust and that select residues in the structure are responsible for i) defense against auto-oxidation and bleaching, ii) amino acid mediated electron-transfer pathways, iii) the stabilization of substrate interactions, and iv) serving as acid/base catalysts. Thus, structure–function relationships, albeit subtle, exist in DHP, and through specific mutations certain relationships can be selectively tuned or exploited.

4.3. Multispecificity and active site flexibility

Substrate functionalization using the same oxidative function, e.g., peroxidase activity employed in the oxidation of halophenols, guaiacols and cresols, allows for DHP to be classified as a multi-specific enzyme. This broad specificity, also referred to as substrate promiscuity, translates into a flexible active site that accommodates a variety of substrates [65,151,152]. The active site of DHP is close to the surface of the protein scaffold, thus rendering it more solvent exposed when compared to other enzymes such as CYP450 and UPOs. Additionally, the active site is largely composed of hydrophobic amino acid residues, and enzyme-substrate hydrophobic interactions (in addition to hydrogen bonding and electrostatic interactions) are an important driving force stabilizing substrate binding, which in turn facilitates the formation of the enzyme-substrate transition states [153,154].

The previously determined crystal structures of 2,4,6-TCP and 2,4,6-TBP [26,85] (Fig. 14A) were superimposed with 5-Br-I, 4-Br-C, 4-NP, and *p*-cresol (Fig. 14B and C) in order to directly compare and understand the structural interactions of the distal cavity of DHP. As mentioned previously, 2,4,6-TCP has two different binding sites in the distal cavity of DHP, internal and external. TCP_{int} is buried in the distal pocket (close to the α heme edge), the *para*-halogen atom is located in the Xe1 hydrophobic cavity and the hydroxyl group is 4.6 Å away from the heme iron and interacts with H55 in the closed conformation (N^{ε} 2.7 Å). TCP_{ext} is positioned close to the entrance of the distal pocket (γ edge), and the hydroxyl group interacts with H55 in the open conformation (OH-N^{δ} 2.5 Å) and Y38 (OH-OH, 2.7 Å). The chlorine atom in the *para*-position is at a distance of 3.3 Å from the heme iron [26]. The brominated derivative, 2,4,6-TBP, also binds internally with the *para*-halogen atom located in the Xe1 hydrophobic cavity but positioned a little deeper compared to TCP_{int} because of its size and hydrophobic interactions. The TBP hydroxyl group is farther away from H55 (N^{ε} 5.3 Å) due to its position pointing down towards the heme iron (Fe-OH, 3.6 Å) [85].

The binding mode of TBP and TCP_{int} is slightly rotated relative to each other (Fig. 14**A**), owing to the aromatic ring planes being angled at approximately 59.8° resulting in the 6-position halogens being separated by 4.6 Å (not shown). The Br in position 6 is oriented towards a more hydrophobic region of the pocket, in proximity to V59, M63 and L100, whereas the Cl in the same position is rotated toward F21, F60, but also pointing towards a carbonyl oxygen of T56 (Cl to C=O is 3.8 Å) (not shown). The halogens in the 2- and 4-positions occupy the overlapping space in the Xe1 binding cavity, with the Br in position 4 being positioned a little deeper due to its size and hydrophobic interactions (mutual distance of 0.4 and 0.7 Å, respectively).

The superimposed structures of the substrates that bind internally, 2,4,6-TCP_{int} (cyan) [26], 2,4,6-TBP (pink) [85], 4-Br-C (green) [7] and, 5-Br-I (magenta) [49] are shown in Fig. 14B. H55 is shown in both the open and closed conformation, where the substrates interact with N^{ε} of H55 (closed conformation), with distances that range from 2.5 to 2.9 Å (except TBP, 5.3 Å). The halogen atom of all

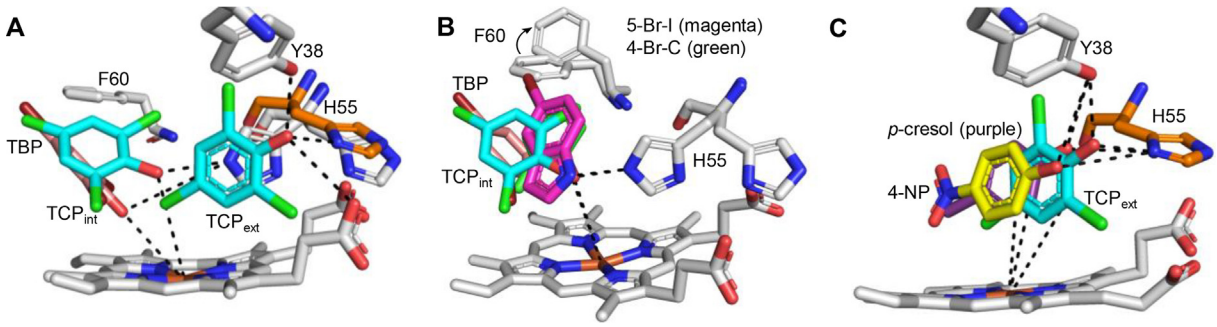

Fig. 14. Superimposed crystal structures of dehaloperoxidase, as seen from the δ edge, complexed with A) 2,4,6-TCP (TCP_{int}, PDB: 4KMV; TCP_{ext}, PDB: 4KMW) and 2,4,6-TBP (PDB: 4ILZ), B) 5-bromoindole (PDB: 6I6G, magenta), 4-bromo-*o*-cresol (PDB: 6ONX, green), TCP_{int}, (PDB: 4KMV, cyan) and 2,4,6-TBP (PDB: 4ILZ, pink), and C) 4-nitrophenol (PDB: 5CHQ, yellow), *p*-cresol (PDB: 6OO6, purple) and TCP_{ext} (PDB: 4KMW, cyan).

substrates is in the Xe1 hydrophobic cavity, albeit in slightly different positions. The structures show 5-Br-I and 4-Br-C in near perfect overlap (0.5 Å displacement between the Br atoms, and 0.2 Å between the phenolic oxygen and indole nitrogen), with an identical distance from the heme iron and N^{ε} of H55 to either the indole nitrogen in 5-Br-I or the phenolic oxygen of 4-Br-C (4.8 Å and 2.5 Å, respectively). The residue F60 was displaced for 5-Br-I and 4-Br-C to a "open" conformation, possibly to accommodate the bulky halogen atom for both these substrates (Fig. 14B). Other residues F21, F24, F35, L100 and V59 were found to be in slightly different conformations for all four substrates, while still positioned to stabilize the substrates via hydrophobic interactions (not shown). The residues Y38 and T56 do not have interactions with these substrates [7,26,49,85].

Conversely, 2,4,6-TCP_{ext} (cyan) [26], 4-NP (yellow) [10] and, *p*-cresol (purple) [7] bind closer to the entrance of the pocket (γ edge), and thus are more solvent exposed (Fig. 14**C**). All three substrates are positioned almost perpendicular to the heme cofactor, H55 is in the open conformation in all three structures, and the hydroxyl group of the substrates, which points towards the γ edge, interacts with N^{δ} with distances ranging from 2.5 to 4.9 Å. In addition, the distance between C2 and the iron center is 4.5 Å for *p*-cresol and 4-NP, which provides an explanation for hydroxylation in this position. Even though the distance between C2 and the iron center is 5.7 Å for TCP_{ext}, this carbon is sterically hindered for this substrate. The residues F21, F24, F35, F60, L100 and V59 were found to be in slightly different conformations for all four substrates, while still positioned to stabilize the substrates via hydrophobic interactions (not shown). The substrates interact with Y38 (2.7 Å for TCP and 4-NP; 3.8 Å for *p*-cresol) and both 4-NP and *p*-cresol interact with the propionate group D (2.6 and 3.1 Å, respectively). Lastly, *p*-cresol interacts with T56 (3.8 Å, not shown).

In summary, different structural aspects were found to affect the substrate binding position and affinity to the protein, and although subtly in DHP, they represent key contributions that are likely applied by the enzyme to differentiate between functions. Some of these can be summarized as i) proximity to the iron center and availability for O-atom transfer, ii) enhanced conformational flexibility, where small side chain rearrangements of select amino acids (e.g., open or closed conformation of H55, or displacement of F60) and/or substrate binding position (e.g., internal or external) in the pocket can play a role in substrate specificity; ii) hydrophobic interactions that bind and stabilize the substrate in the active site and, iii) hydrogen bonding interactions, affected by different protonation sites within the distal cavity [153,154].

5. Final remarks

The investigation of enzymes with promiscuous activities, where protein engineering and directed evolution offer the means to achieving the desired non-native functions, has been the focus of many research groups. However, such experiments are often laborious, time consuming, and costly. As a potential protein engineering platform, the enzyme known as dehaloperoxidase-hemoglobin has provided us with a recent example of a multifunctional enzyme that has the potential to significantly advance our understanding of the protein structure–function correlation. Of course, structure is related to function, but the question is whether, or how, structure uniquely defines function. In DHP, it appears that the substrate itself plays a pivotal role in determining which activity (peroxidase, peroxygenase, oxidase and/or oxygenase) the enzyme performs. Altogether, this intriguing functional switch in the presence of different substrates may be triggered by the physical or electronic properties of the substrate, its binding orientation in the active site, or by a change in the protein's redox properties. In essence, the various substrates alter the enzymatic function of the catalytic globin in much the same way allosteric effectors would structurally shift the equilibrium of a cooperative hemoglobin. Thus, DHP provides a unique and advantageous platform for deeply probing mechanistic questions related to the protein environment: by simply changing the substrate, the unique set of protein-substrate interactions specific to each of the five different heme activities of DHP can be studied, enabling us to pose questions related to multiple activities across the heme protein superfamily using just a single enzyme. Moreover, the relationship of DHP to other hemoglobins, peroxidases and peroxygenases aids in establishing new paradigms of protein structure–function relationships relevant to multifunctional proteins, complementing those established for monofunctional enzymes. More broadly, the knowledge gained through the studies performed on DHP over the past two decades advances our understanding of catalytic globins, helps to elaborate the structural features that lead to activity differentiation across heme proteins (and across metalloenzymes more generally), and furthers the comparison of the structure–function correlation in enzymes of marine origin in relation to terrestrial or bacterial ones.

Declaration of Competing Interest

The authors declare that they have no known competing financial interests or personal relationships that could have appeared to influence the work reported in this paper.

Acknowledgements

This project was funded by the National Science Foundation (CHE-1609446 and CHE-2002954). The authors would like to thank Dr. Vesna de Serrano, Dr. Joshua Kyle Stanfield and Dr. Evan E. Beauvilliers for their invaluable contributions.

References

[1] R.E. Weber, C. Mangum, H. Steinman, C. Bonaventura, B. Sullivan, J. Bonaventura, Hemoglobins of two terebellid polychaetes: *Enoplobranchus sanguineus* and *Amphitrite ornata*, Comp. Biochem. Physiol. A Comp. Physiol. 56 (1977) 179–187, https://doi.org/10.1016/0300-9629(77)90182-7.

[2] Y.P. Chen, S.A. Woodin, D.E. Lincoln, C.R. Lovell, An unusual dehalogenating peroxidase from the marine terebellid polychaete *Amphitrite ornata*, J. Biol. Chem. 271 (1996) 4609–4612, https://doi.org/10.1074/jbc.271.9.4609.

[3] D.E. Lincoln, K.T. Fielman, R.L. Marinelli, S.A. Woodin, Bromophenol accumulation and sediment contamination by the marine annelids *Notomastus lobatus* and *Thelepus crispus*, Biochem. Syst. Ecol. 33 (2005) 559–570, https://doi.org/10.1016/j.bse.2004.12.006.

[4] S. Franzen, R.A. Ghiladi, L. Lebioda, J. Dawson, Chapter 10 Multi-functional Hemoglobin Dehaloperoxidases, in: Heme Peroxidases, The Royal Society of Chemistry 2016, pp. 218-244. https://doi.org/10.1039/9781782622628-00218.

[5] L. Lebioda, M.W. LaCount, E. Zhang, Y.P. Chen, K. Han, M.M. Whitton, D.E. Lincoln, S.A. Woodin, An enzymatic globin from a marine worm, Nature 401 (1999) 445, https://doi.org/10.1038/46728.

[6] A.H. McGuire, L.M. Carey, V. de Serrano, S. Dali, R.A. Ghiladi, Peroxidase versus peroxygenase activity: Substrate substituent effects as modulators of enzyme function in the multifunctional catalytic globin dehaloperoxidase, Biochemistry 57 (2018) 4455–4468, https://doi.org/10.1021/acs.biochem.8b00540.

[7] T. Malewschik, V. de Serrano, A.H. McGuire, R.A. Ghiladi, The multifunctional globin dehaloperoxidase strikes again: Simultaneous peroxidase and peroxygenase mechanisms in the oxidation of EPA pollutants, Arch. Biochem. Biophys. 673 (2019), https://doi.org/10.1016/j.abb.2019.108079 108079.

[8] D.A. Barrios, J. D'Antonio, N.L. McCombs, J. Zhao, S. Franzen, A.C. Schmidt, L.A. Sombers, R.A. Ghiladi, Peroxygenase and oxidase activities of dehaloperoxidase-hemoglobin from *Amphitrite ornata*, J. Am. Chem. Soc. 136 (2014) 7914–7925, https://doi.org/10.1021/ja500293c.

[9] N.L. McCombs, Unraveling the Multiple Enzymatic Activities of the Dehaloperoxidase-Hemoglobin from Amphitrite ornata, Chemistry, PhD (2017).

[10] N.L. McCombs, J. D'Antonio, D.A. Barrios, L.M. Carey, R.A. Ghiladi, Nonmicrobial Nitrophenol Degradation via Peroxygenase Activity of

Dehaloperoxidase-Hemoglobin from *Amphitrite ornata*, Biochemistry 55 (2016) 2465–2478, https://doi.org/10.1021/acs.biochem.6b00143.
[11] N.L. McCombs, T. Smirnova, R.A. Ghiladi, Oxidation of pyrrole by dehaloperoxidase-hemoglobin: chemoenzymatic synthesis of pyrrolin-2-ones, Catal. Sci. Technol. 7 (2017) 3104–3118, https://doi.org/10.1039/c7cy00781g.
[12] M.P. Roach, Y.P. Chen, S.A. Woodin, D.E. Lincoln, C.R. Lovell, J.H. Dawson, *Notomastus lobatus* chloroperoxidase and *Amphitrite ornata* dehaloperoxidase both contain histidine as their proximal heme iron ligand, Biochemistry 36 (1997) 2197–2202, https://doi.org/10.1021/bi9621371.
[13] S. Franzen, M.P. Roach, Y.P. Chen, R.B. Dyer, W.H. Woodruff, J.H. Dawson, The unusual reactivities of *Amphirite ornata* dehaloperoxidase and *Notomastus lobatus* chloroperoxidase do not arise from a histidine imidazolate proximal heme iron ligand, J. Am. Chem. Soc. 120 (1998) 4658–4661, https://doi.org/10.1021/ja973212d.
[14] H. Ma, M.K. Thompson, J. Gaff, S. Franzen, Kinetic analysis of a naturally occurring bioremediation enzyme: Dehaloperoxidase-hemoglobin from Amphitrite ornata, J. Phys. Chem. B 114 (2010) 13823–13829, https://doi.org/10.1021/jp1014516.
[15] R. Davydov, R.L. Osborne, M. Shanmugam, J. Du, J.H. Dawson, B.M. Hoffman, Probing the oxyferrous and catalytically active ferryl states of *Amphitrite ornata* dehaloperoxidase by cryoreduction and EPR/ENDOR spectroscopy. Detection of compound I, J. Am. Chem. Soc. 132 (2010) 14995–15004, https://doi.org/10.1021/ja1059747.
[16] J. Du, M. Sono, J.H. Dawson, Functional switching of *Amphitrite ornata* dehaloperoxidase from O_2-binding globin to peroxidase enzyme facilitated by halophenol substrate and H_2O_2, Biochemistry 49 (2010) 6064–6069, https://doi.org/10.1021/bi100741z.
[17] J. D'Antonio, E.L. D'Antonio, M.K. Thompson, E.F. Bowden, S. Franzen, T. Smirnova, R.A. Ghiladi, Spectroscopic and mechanistic investigations of dehaloperoxidase B from *Amphitrite ornata*, Biochemistry 49 (2010) 6600–6616, https://doi.org/10.1021/bi100407v.
[18] M.K. Thompson, S. Franzen, R.A. Ghiladi, B.J. Reeder, D.A. Svistunenko, Compound ES of dehaloperoxidase decays via two alternative pathways depending on the conformation of the distal histidine, J. Am. Chem. Soc. 132 (2010) 17501–17510, https://doi.org/10.1021/ja106620q.
[19] J. D'Antonio, R.A. Ghiladi, Reactivity of deoxy- and oxyferrous dehaloperoxidase B from *Amphitrite ornata*: Identification of compound II and its ferrous-hydroperoxide precursor, Biochemistry 50 (2011) 5999–6011, https://doi.org/10.1021/bi200311u.
[20] J. Du, X. Huang, S. Sun, C. Wang, L. Lebioda, J.H. Dawson, *Amphitrite ornata* Dehaloperoxidase (DHP): Investigations of structural factors that influence the mechanism of halophenol dehalogenation using "peroxidase-like" myoglobin mutants and "myoglobin-like" DHP mutants, Biochemistry 50 (2011) 8172–8180, https://doi.org/10.1021/bi2009129.
[21] L. Szatkowski, M.K. Thompson, R. Kaminski, S. Franzen, A. Dybala-Defratyka, Oxidative dechlorination of halogenated phenols catalyzed by two distinct enzymes: Horseradish peroxidase and dehaloperoxidase, Arch. Biochem. Biophys. 505 (2011) 22–32, https://doi.org/10.1016/j.abb.2010.09.018.
[22] S. Franzen, M.K. Thompson, R.A. Ghiladi, The dehaloperoxidase paradox, Biochim. Biophys. Acta 2012 (1824) 578–588, https://doi.org/10.1016/j.bbapap.2011.12.008.
[23] J. Zhao, V. de Serrano, R. Dumarieh, M. Thompson, R.A. Ghiladi, S. Franzen, The role of the distal histidine in H_2O_2 activation and heme protection in both peroxidase and globin functions, J. Phys. Chem. B 116 (2012) 12065–12077, https://doi.org/10.1021/jp300014b.
[24] R.L. Osborne, L.O. Taylor, K.P. Han, B. Ely, J.H. Dawson, *Amphitrite ornata* dehaloperoxidase: enhanced activity for the catalytically active globin using MCPBA, Biochem. Biophys. Res. Commun. 324 (2004) 1194–1198, https://doi.org/10.1016/j.bbrc.2004.09.174.
[25] R. Dumarieh, J. D'Antonio, A. Deliz-Liang, T. Smirnova, D.A. Svistunenko, R.A. Ghiladi, Tyrosyl radicals in dehaloperoxidase: How nature deals with evolving an oxygen-binding globin to a biologically relevant peroxidase, J. Biol. Chem. 288 (2013) 33470–33482, https://doi.org/10.1074/jbc.M113.496497.
[26] C. Wang, L.L. Lovelace, S. Sun, J.H. Dawson, L. Lebioda, Complexes of dual-function hemoglobin/dehaloperoxidase with substrate 2,4,6-trichlorophenol are inhibitory and indicate binding of halophenol to compound I, Biochemistry 52 (2013) 6203–6210, https://doi.org/10.1021/bi400627w.
[27] S. Sun, M. Sono, J. Du, J.H. Dawson, Evidence of the direct involvement of the substrate TCP radical in functional switching from oxyferrous O_2 carrier to ferric peroxidase in the dual-function hemoglobin/dehaloperoxidase from *Amphitrite ornata*, Biochemistry 53 (2014) 4956–4969, https://doi.org/10.1021/bi5002757.
[28] S. Sun, M. Sono, C. Wang, J. Du, L. Lebioda, J.H. Dawson, Influence of heme environment structure on dioxygen affinity for the dual function *Amphitrite ornata* hemoglobin/dehaloperoxidase. Insights into the evolutional structure–function adaptations, Arch. Biochem. Biophys. 545 (2014) 108–115, https://doi.org/10.1016/j.abb.2014.01.010.
[29] J. Belyea, L.B. Gilvey, M.F. Davis, M. Godek, T.L. Sit, S.A. Lommel, S. Franzen, Enzyme function of the globin dehaloperoxidase from Amphitrite ornata is activated by substrate binding, Biochemistry 44 (2005) 15637–15644, https://doi.org/10.1021/bi051731k.
[30] R.L. Osborne, S. Sumithran, M.K. Coggins, Y.P. Chen, D.E. Lincoln, J.H. Dawson, Spectroscopic characterization of the ferric states of *Amphitrite ornata* dehaloperoxidase and *Notomastus lobatus* chloroperoxidase: His-ligated peroxidases with globin-like proximal and distal properties, J. Inorg. Biochem. 100 (2006) 1100–1108, https://doi.org/10.1016/j.jinorgbio.2006.02.008.
[31] T.I. Smirnova, R.T. Weber, M.F. Davis, S. Franzen, Substrate binding triggers a switch in the iron coordination in dehaloperoxidase from *Amphitrite ornata*: HYSCORE experiments, J. Am. Chem. Soc. 130 (2008) 2128–2129, https://doi.org/10.1021/ja0772952.
[32] R. Davydov, R.L. Osborne, S.H. Kim, J.H. Dawson, B.M. Hoffman, EPR and ENDOR studies of cryoreduced compounds II of peroxidases and myoglobin. Proton-coupled electron transfer and protonation status of ferryl hemes, Biochemistry 47 (2008) 5147–5155, https://doi.org/10.1021/bi702514d.
[33] J. Feducia, R. Dumarieh, L.B. Gilvey, T. Smirnova, S. Franzen, R.A. Ghiladi, Characterization of dehaloperoxidase compound ES and its reactivity with trihalophenols, Biochemistry 48 (2009) 995–1005, https://doi.org/10.1021/bi801916j.
[34] R.L. Osborne, M.K. Coggins, G.M. Raner, M. Walla, J.H. Dawson, The mechanism of oxidative halophenol dehalogenation by *Amphitrite ornata* dehaloperoxidase is initiated by H_2O_2 binding and involves two consecutive one-electron steps: role of ferryl intermediates, Biochemistry 48 (2009) 4231–4238, https://doi.org/10.1021/bi900367e.
[35] M.F. Davis, H. Gracz, F.A. Vendeix, V. de Serrano, A. Somasundaram, S.M. Decatur, S. Franzen, Different modes of binding of mono-, di-, and trihalogenated phenols to the hemoglobin dehaloperoxidase from *Amphitrite ornata*, Biochemistry 48 (2009) 2164–2172, https://doi.org/10.1021/bi801568s.
[36] L.M. Carey, R. Gavenko, D.A. Svistunenko, R.A. Ghiladi, How nature tunes isoenzyme activity in the multifunctional catalytic globin dehaloperoxidase from Amphitrite ornata, Biochim. Biophys. Acta 2018 (1866) 230–241, https://doi.org/10.1016/j.bbapap.2017.11.004.
[37] S. Franzen, K. Sasan, B.E. Sturgeon, B.J. Lyon, B.J. Battenburg, H. Gracz, R. Dumariah, R. Ghiladi, Nonphotochemical base-catalyzed hydroxylation of 2,6-dichloroquinone by H_2O_2 occurs by a radical mechanism, J. Phys. Chem. B 116 (2012) 1666–1676, https://doi.org/10.1021/jp208536x.
[38] K. Han, S.A. Woodin, D.E. Lincoln, K.T. Fielman, B. Ely, *Amphitrite ornata*, a marine worm, contains two dehaloperoxidase genes, Mar. Biotechnol. NY 3 (2001) 287–292, https://doi.org/10.1007/s10126-001-0003-8.
[39] G.W. Gribble, The diversity of naturally occurring organobromine compounds, Chem. Soc. Rev. 28 (1999) 335–346, https://doi.org/10.1039/A900201d.
[40] G.W. Gribble, The natural production of organobromine compounds, Environ. Sci. Pollut. Res. Int. 7 (2000) 37–47, https://doi.org/10.1065/espr199910.002.
[41] T.L. Poulos, J. Kraut, The stereochemistry of peroxidase catalysis, J. Biol. Chem. 255 (1980) 8199–8205, https://doi.org/10.1016/S0021-9258(19)70630-9.
[42] T.L. Poulos, Thirty years of heme peroxidase structural biology, Arch Biochem Biophys 500 (2010) 3–12, https://doi.org/10.1016/j.abb.2010.02.008.
[43] M.W. LaCount, E. Zhang, Y.P. Chen, K. Han, M.M. Whitton, D.E. Lincoln, S.A. Woodin, L. Lebioda, The crystal structure and amino acid sequence of dehaloperoxidase from *Amphitrite ornata* indicate common ancestry with globins, J. Biol. Chem. 275 (2000) 18712–18716, https://doi.org/10.1074/jbc.M001194200.
[44] V. de Serrano, J. D'Antonio, S. Franzen, R.A. Ghiladi, Structure of dehaloperoxidase B at 1.58 A resolution and structural characterization of the AB dimer from *Amphitrite ornata*, Acta Cryst. D 66 (2010) 529–538, https://doi.org/10.1107/S0907444910004580.
[45] Z. Chen, V. de Serrano, L. Betts, S. Franzen, Distal histidine conformational flexibility in dehaloperoxidase from *Amphitrite ornate*, Acta Cryst. D 65 (2009) 34–40, https://doi.org/10.1107/S0907444908036548.
[46] E. Zhang, Y.P. Chen, M.P. Roach, D.E. Lincoln, C.R. Lovell, S.A. Woodin, J.H. Dawson, L. Lebioda, Crystallization and initial spectroscopic characterization of the heme-containing dehaloperoxidase from the marine polychaete *Amphitrite ornata*, Acta Crystallogr. D Biol. Crystallogr. 52 (1996) 1191–1193, https://doi.org/10.1107/S0907444996007974.
[47] V. de Serrano, S. Franzen, Structural evidence for stabilization of inhibitor binding by a protein cavity in the dehaloperoxidase-hemoglobin from *Amphitrite ornata*, Biopolymers 98 (2012) 27–35, https://doi.org/10.1002/bip.21674.
[48] M.K. Thompson, M.F. Davis, V. de Serrano, F.P. Nicoletti, B.D. Howes, G. Smulevich, S. Franzen, Internal binding of halogenated phenols in dehaloperoxidase-hemoglobin inhibits peroxidase function, Biophys. J. 99 (2010) 1586–1595, https://doi.org/10.1016/j.bpj.2010.05.041.
[49] T. Moreno-Chicano, A. Ebrahim, D. Axford, M.V. Appleby, J.H. Beale, A.K. Chaplin, H.M.E. Duyvesteyn, R.A. Ghiladi, S. Owada, D.A. Sherrell, R.W. Strange, H. Sugimoto, K. Tono, J.A.R. Worrall, R.L. Owen, M.A. Hough, High-throughput structures of protein-ligand complexes at room temperature using serial femtosecond crystallography, IUCrJ 6 (2019) 1074–1085, https://doi.org/10.1107/S2052252519011655.
[50] N.L. McCombs, T. Moreno-Chicano, L.M. Carey, S. Franzen, M.A. Hough, R.A. Ghiladi, Interaction of azole-based environmental pollutants with the Coelomic hemoglobin from Amphitrite ornata: A molecular basis for toxicity, Biochemistry 56 (2017) 2294–2303, https://doi.org/10.1021/acs.biochem.7b00041.
[51] S. Jiang, I. Wright, P. Swartz, S. Franzen, The role of T56 in controlling the flexibility of the distal histidine in dehaloperoxidase-hemoglobin from *Amphitrite ornata*, BBA-Proteins Proteom. 2013 (1834) 2020–2029, https://doi.org/10.1016/j.bbapap.2013.06.005.

[52] E.L. D'Antonio, J. D'Antonio, V. de Serrano, H. Gracz, M.K. Thompson, R.A. Ghiladi, E.F. Bowden, S. Franzen, Functional consequences of the creation of an Asp-His-Fe triad in a 3/3 globin, Biochemistry 50 (2011) 9664–9680, https://doi.org/10.1021/bi201368u.
[53] E.G. Hrycay, S.M. Bandiera, Monooxygenase, peroxidase and peroxygenase properties and reaction mechanisms of cytochrome P450 enzymes, Adv. Exp. Med. Biol. 851 (2015) 1–61, https://doi.org/10.1007/978-3-319-16009-2.
[54] Y. Wang, D. Lan, R. Durrani, F. Hollmann, Peroxygenases en route to becoming dream catalysts. What are the opportunities and challenges?, Curr. Opin. Chem. Biol. 37 (2017) 1–9, https://doi.org/10.1016/j.cbpa.2016.10.007.
[55] S. Bormann, A. Gomez Baraibar, Y. Ni, D. Holtmann, F. Hollmann, Specific oxyfunctionalisations catalysed by peroxygenases: opportunities, challenges and solutions, Catal. Sci. Technol., 5 (2015) 2038–2052. https://doi.org/10.1039/c4cy01477d.
[56] M. Hofrichter, R. Ullrich, Oxidations catalyzed by fungal peroxygenases, Curr. Opin. Chem. Biol. 19 (2014) 116–125, https://doi.org/10.1016/j.cbpa.2014.01.015.
[57] O. Shoji, Y. Watanabe, Peroxygenase reactions catalyzed by cytochromes P450, J. Biol. Inorg. Chem. 19 (2014) 529–539, https://doi.org/10.1007/s00775-014-1106-9.
[58] N. Ma, Z. Chen, J. Chen, J. Chen, C. Wang, H. Zhou, L. Yao, O. Shoji, Y. Watanabe, Z. Cong, Dual-functional small molecules for generating an efficient cytochrome P450BM3 peroxygenase, Angew. Chem. Int. Ed. Engl. 57 (2018) 7628–7633, https://doi.org/10.1002/anie.201801592.
[59] A.W. Munro, K.J. McLean, J.L. Grant, T.M. Makris, Structure and function of the cytochrome P450 peroxygenase enzymes, Biochem. Soc. Trans. 46 (2018) 183–196, https://doi.org/10.1042/BST20170218.
[60] H.M. Girvan, H. Poddar, K.J. McLean, D.R. Nelson, K.A. Hollywood, C.W. Levy, D. Leys, A.W. Munro, Structural and catalytic properties of the peroxygenase P450 enzyme CYP152K6 from Bacillus methanolicus, J. Inorg. Biochem. 188 (2018) 18–28, https://doi.org/10.1016/j.jinorgbio.2018.08.002.
[61] H. Onoda, O. Shoji, K. Suzuki, H. Sugimoto, Y. Shiro, Y. Watanabe, α-Oxidative decarboxylation of fatty acids catalysed by cytochrome P450 peroxygenases yielding shorter-alkyl-chain fatty acids, Catal. Sci. Technol. 8 (2018) 434–442, https://doi.org/10.1039/c7cy02263h.
[62] M. Hobisch, D. Holtmann, P. Gomez de Santos, M. Alcalde, F. Hollmann, S. Kara, Recent developments in the use of peroxygenases – Exploring their high potential in selective oxyfunctionalisations, Biotechnol. Adv. (2020), https://doi.org/10.1016/j.biotechadv.2020.107615 107615.
[63] S. Peter, M. Kinne, R. Ullrich, G. Kayser, M. Hofrichter, Epoxidation of linear, branched and cyclic alkenes catalyzed by unspecific peroxygenase, Enzyme Microb. Technol. 52 (2013) 370–376, https://doi.org/10.1016/j.enzmictec.2013.02.013.
[64] A.T. Martinez, F.J. Ruiz-Duenas, S. Camarero, A. Serrano, D. Linde, H. Lund, J. Vind, M. Tovborg, O.M. Herold-Majumdar, M. Hofrichter, C. Liers, R. Ullrich, K. Scheibner, G. Sannia, A. Piscitelli, C. Pezzella, M.E. Sener, S. Kilic, W.J.H. van Berkel, V. Guallar, M.F. Lucas, R. Zuhse, R. Ludwig, F. Hollmann, E. Fernandez-Fueyo, E. Record, C.B. Faulds, M. Tortajada, I. Winckelmann, J.A. Rasmussen, M. Gelo-Pujic, A. Gutierrez, J.C. Del Rio, J. Rencoret, M. Alcalde, Oxidoreductases on their way to industrial biotransformations, Biotechnol. Adv. 35 (2017) 815–831, https://doi.org/10.1016/j.biotechadv.2017.06.003.
[65] M. Ramirez-Escudero, P. Molina-Espeja, P. Gomez de Santos, M. Hofrichter, J. Sanz-Aparicio, M. Alcalde, Structural insights into the substrate promiscuity of a laboratory-evolved peroxygenase, ACS Chem. Biol. 13 (2018) 3259–3268, https://doi.org/10.1021/acschembio.8b00500.
[66] M. Faiza, S. Huang, D. Lan, Y. Wang, New insights on unspecific peroxygenases: superfamily reclassification and evolution, BMC Evol. Biol. 19 (2019) 76, https://doi.org/10.1186/s12862-019-1394-3.
[67] A. Karich, R. Ullrich, K. Scheibner, M. Hofrichter, Fungal unspecific peroxygenases oxidize the majority of organic EPA priority pollutants, Front. Microbiol. 8 (2017) 1463, https://doi.org/10.3389/fmicb.2017.01463.
[68] K. Piontek, E. Strittmatter, R. Ullrich, G. Grobe, M.J. Pecyna, M. Kluge, K. Scheibner, M. Hofrichter, D.A. Plattner, Structural basis of substrate conversion in a new aromatic peroxygenase: Cytochrome P450 functionality with benefits, J. Biol. Chem. 288 (2013) 34767–34776, https://doi.org/10.1074/jbc.M113.514521.
[69] X. Huang, J.T. Groves, Oxygen activation and radical transformations in Heme proteins and Metalloporphyrins, Chem. Rev. 118 (2018) 2491–2553, https://doi.org/10.1021/acs.chemrev.7b00373.
[70] S. Matthews, J.D. Belcher, K.L. Tee, H.M. Girvan, K.J. McLean, S.E. Rigby, C.W. Levy, D. Leys, D.A. Parker, R.T. Blankley, A.W. Munro, Catalytic Determinants of Alkene Production by the Cytochrome P450 Peroxygenase OleTJE, J. Biol. Chem. 292 (2017) 5128–5143, https://doi.org/10.1074/jbc.M116.762336.
[71] J.A. Amaya, C.D. Rutland, T.M. Makris, Mixed regiospecificity compromises alkene synthesis by a cytochrome P450 peroxygenase from Methylobacterium populi, J Inorg Biochem 158 (2016) 11–16, https://doi.org/10.1016/j.jinorgbio.2016.02.031.
[72] A.S. Faponle, M.G. Quesne, S.P. de Visser, Origin of the regioselective fatty-acid hydroxylation versus decarboxylation by a cytochrome P450 peroxygenase: What drives the reaction to biofuel production?, Chemistry 22 (2016) 5478–5483, https://doi.org/10.1002/chem.201600739.
[73] P.L. Thomas, Peroxidases, Curr. Opin. Biotechnol. 4 (1993) 484–489, https://doi.org/10.1016/0958-1669(93)90016-P.
[74] L. Banci, Structural properties of peroxidases, J. Biotechnol. 53 (1997) 253–263, https://doi.org/10.1016/S0168-1656(97)01677-5.
[75] J.H. Dawson, Probing structure-function relations in Heme-containing oxygenases and peroxidases, Science 240 (1988) 433–439, https://doi.org/10.1126/science.3358128.
[76] H.B. Dunford, J.S. Stillman, On the function and mechanism of action of peroxidases, Coord. Chem. Rev. 19 (1976) 187–251, https://doi.org/10.1016/S0010-8545(00)80316-1.
[77] X. Wang, R. Ullrich, M. Hofrichter, J.T. Groves, Heme-thiolate ferryl of aromatic peroxygenase is basic and reactive, Proc. Natl. Acad. Sci. U.S.A. 112 (2015) 3686–3691, https://doi.org/10.1073/pnas.1503340112.
[78] O. Shoji, C. Wiese, T. Fujishiro, C. Shirataki, B. Wunsch, Y. Watanabe, Aromatic C-H bond hydroxylation by P450 peroxygenases: a facile colorimetric assay for monooxygenation activities of enzymes based on Russig's blue formation, J. Biol. Inorg. Chem. 15 (2010) 1109–1115, https://doi.org/10.1007/s00775-010-0671-9.
[79] X. Huang, J.T. Groves, Beyond ferryl-mediated hydroxylation: 40 years of the rebound mechanism and C-H activation, J. Biol. Inorg. Chem. 22 (2017) 185–207, https://doi.org/10.1007/s00775-016-1414-3.
[80] F.G. Bordwell, Equilibrium acidities in dimethyl sulfoxide solution, Acc. Chem. Res. 21 (1988) 456–463, https://doi.org/10.1021/ar00156a004.
[81] J.M. Mayer, Understanding hydrogen atom transfer: From bond strengths to marcus theory, Acc. Chem. Res. 44 (2011) 36–46, https://doi.org/10.1021/ar100093z.
[82] J.J. Warren, T.A. Tronic, J.M. Mayer, Thermochemistry of proton-coupled electron transfer reagents and its implications, Chem. Rev. 110 (2010) 6961–7001, https://doi.org/10.1021/cr100085k.
[83] J.T. Groves, Enzymatic C-H bond activation: Using push to get pull, Nat. Chem. 6 (2014) 89–91, https://doi.org/10.1038/nchem.1855.
[84] J.K. Stanfield, K. Omura, A. Matsumoto, C. Kasai, H. Sugimoto, Y. Shiro, Y. Watanabe, O. Shoji, Crystals in minutes: Instant on-site microcrystallisation of various flavours of the CYP102A1 (P450BM3) Haem domain, Angew. Chem. Int. Ed. Engl. 59 (2020) 7611–7618, https://doi.org/10.1002/anie.201913407.
[85] J. Zhao, V. de Serrano, P. Le, S. Franzen, Structural and kinetic study of an internal substrate binding site in dehaloperoxidase-hemoglobin A from *Amphitrite ornata*, Biochemistry 52 (2013) 2427–2439, https://doi.org/10.1021/bi301307f.
[86] E.M. Gillam, A.M. Aguinaldo, L.M. Notley, D. Kim, R.G. Mundkowski, A.A. Volkov, F.H. Arnold, P. Soucek, J.J. DeVoss, F.P. Guengerich, Formation of indigo by recombinant mammalian cytochrome P450, Biochem. Biophys. Res. Commun. 265 (1999) 469–472, https://doi.org/10.1006/bbrc.1999.1702.
[87] E.M. Gillam, F.P. Guengerich, Exploiting the versatility of human cytochrome P450 enzymes: the promise of blue roses from biotechnology, IUBMB Life 52 (2001) 271–277, https://doi.org/10.1080/152165401317291110.
[88] E.M. Gillam, L.M. Notley, H. Cai, J.J. De Voss, F.P. Guengerich, Oxidation of indole by cytochrome P450 enzymes, Biochemistry 39 (2000) 13817–13824, https://doi.org/10.1021/bi001229u.
[89] K. Nakamura, M.V. Martin, F.P. Guengerich, Random mutagenesis of human cytochrome p450 2A6 and screening with indole oxidation products, Arch. Biochem. Biophys. 395 (2001) 25–31, https://doi.org/10.1006/abbi.2001.2569.
[90] J. Kim, P.G. Lee, E.O. Jung, B.G. Kim, In vitro characterization of CYP102G4 from Streptomyces cattleya: A self-sufficient P450 naturally producing indigo, Biochim. Biophys. Acta Proteins Proteom. 2018 (1866) 60–67, https://doi.org/10.1016/j.bbapap.2017.08.002.
[91] Q.S. Li, J. Ogawa, R.D. Schmid, S. Shimizu, Indole hydroxylation by bacterial cytochrome P450 BM-3 and modulation of activity by cumene hydroperoxide, Biosci. Biotechnol. Biochem. 69 (2005) 293–300, https://doi.org/10.1271/bbb.69.293.
[92] H.M. Li, L.H. Mei, V.B. Urlacher, R.D. Schmid, Cytochrome P450 BM-3 evolved by random and saturation mutagenesis as an effective indole-hydroxylating catalyst, Appl. Biochem. Biotechnol. 144 (2008) 27–36, https://doi.org/10.1007/s12010-007-8002-5.
[93] W.C. Huang, A.C. Westlake, J.D. Marechal, M.G. Joyce, P.C. Moody, G.C. Roberts, Filling a hole in cytochrome P450 BM3 improves substrate binding and catalytic efficiency, J. Mol. Biol. 373 (2007) 633–651, https://doi.org/10.1016/j.jmb.2007.08.015.
[94] A.N. Fabara, M.W. Fraaije, An overview of microbial indigo-forming enzymes, Appl. Microbiol. Biotechnol. 104 (2020) 925–933, https://doi.org/10.1007/s00253-019-10292-5.
[95] S.G. Bell, R. Zhou, W. Yang, A.B. Tan, A.S. Gentleman, L.L. Wong, W. Zhou, Investigation of the substrate range of CYP199A4: modification of the partition between hydroxylation and desaturation activities by substrate and protein engineering, Chemistry 18 (2012) 16677–16688, https://doi.org/10.1002/chem.201202776.
[96] T. Furuya, K. Kino, Regioselective oxidation of indole- and quinolinecarboxylic acids by cytochrome P450 CYP199A2, Appl. Microbiol. Biotechnol. 85 (2010) 1861–1868, https://doi.org/10.1007/s00253-009-2207-1.
[97] S. Luo, K. Xu, S. Xiang, J. Chen, C. Chen, C. Guo, Y. Tong, L. Tong, High-resolution structures of inhibitor complexes of human indoleamine 2,3-dioxygenase 1 in a new crystal form, Acta. Crystallogr. F Struct. Biol. Commun. 74 (2018) 717–724, https://doi.org/10.1107/S2053230X18012955.
[98] H. Sugimoto, S. Oda, T. Otsuki, T. Hino, T. Yoshida, Y. Shiro, Crystal structure of human indoleamine 2,3-dioxygenase: catalytic mechanism of O2 incorporation by a heme-containing dioxygenase, Proc. Natl. Acad. Sci. U.S.A. 103 (2006) 2611–2616, https://doi.org/10.1073/pnas.0508996103.

[99] H.H. Kuo, A.G. Mauk, Indole peroxygenase activity of indoleamine 2,3-dioxygenase, Proc. Natl. Acad. Sci. U.S.A. 109 (2012) 13966–13971, https://doi.org/10.1073/pnas.1207191109.
[100] R. Kaur, V. Rani, V. Abbot, Y. Kapoor, D. Konar, K. Kumar, Recent synthetic and medicinal perspectives of pyrroles: An overview, J. Pharm. Chem. Chem. Sci. 1 (2017) 17–32.
[101] F.P. Guengerich, M.B. Mitchell, Metabolic activation of model pyrroles by cytochrome P-450, Drug Metab. Dispos. 8 (1980) 34–38.
[102] R. Cruz-Silva, E. Amaro, A. Escamilla, M.E. Nicho, S. Sepulveda-Guzman, L. Arizmendi, J. Romero-Garcia, F.F. Castillon-Barraza, M.H. Farias, Biocatalytic synthesis of polypyrrole powder, colloids, and films using horseradish peroxidase, J. Colloid Interf. Sci. 328 (2008) 263–269, https://doi.org/10.1016/j.jcis.2008.09.021.
[103] H.-K. Song, G.T.R. Palmore, Conductive polypyrrole via enzyme catalysis, J. Phys. Chem. B 109 (2005) 19278–19287, https://doi.org/10.1021/jp0514978.
[104] C. Schmuck, D. Rupprecht, The synthesis of highly functionalized pyrroles: A challenge in regioselectivity and chemical reactivity, Synthesis 2007 (2007) 3095–3110, https://doi.org/10.1055/s-2007-990783.
[105] in: Title 40 - Protection of Environment, Code of Federal Regulations, Section 423, Appendix A, U.S. Environmental Protection Agency, Washington, D.C., 2013.
[106] W. Tassaneeyakul, M.E. Veronese, D.J. Birkett, J.O. Miners, High-performance liquid chromatographic assay for 4-nitrophenol hydroxylation, a putative cytochrome P-4502E1 activity, in human liver microsomes, J. Chromatogr. B Biomed. Sci. Appl. 616 (1993) 73–78, https://doi.org/10.1016/0378-4347(93)80473-H.
[107] W. Tassaneeyakul, M.E. Veronese, D.J. Birkett, F.J. Gonzalez, J.O. Miners, Validation of 4-nitrophenol as an in vitro substrate probe for human liver CYP2E1 using cDNA expression and microsomal kinetic techniques, Biochem. Pharmacol. 46 (1993) 1975–1981, https://doi.org/10.1016/0006-2952(93)90639-E.
[108] A. Zerilli, D. Ratanasavanh, D. Lucas, T. Goasduff, Y. Dréano, C. Menard, D. Picart, F. Berthou, Both cytochromes P450 2E1 and 3A Are involved in the O-hydroxylation of p-nitrophenol, a catalytic activity known to be specific for P450 2E1, Chem. Res. Toxicol. 10 (1997) 1205–1212, https://doi.org/10.1021/tx970048z.
[109] T.K. Chang, C.L. Crespi, D.J. Waxman, Spectrophotometric analysis of human CYP2E1-catalyzed p-nitrophenol hydroxylation, Methods Mol. Biol. 320 (2006) 127–131, https://doi.org/10.1385/1-59259-998-2:127.
[110] G.M. Raner, J.A. Hatchell, M.U. Dixon, T.L. Joy, A.E. Haddy, E.R. Johnston, Regioselective peroxo-dependent heme alkylation in P450(BM3)-F87G by aromatic aldehydes: effects of alkylation on cataysis, Biochemistry 41 (2002) 9601–9610, https://doi.org/10.1021/bi020256c.
[111] C.J. Whitehouse, S.G. Bell, L.L. Wong, P450(BM3) (CYP102A1): connecting the dots, Chem. Soc. Rev. 41 (2012) 1218–1260, https://doi.org/10.1039/c1cs15192d.
[112] in: Title 15 U.S. Code Chapter 53 - Toxic Substances Control Act, 1976.
[113] M.D. Aitken, I.J. Massey, T. Chen, P.E. Heck, Characterization of reaction products from the enzyme catalyzed oxidation of phenolic pollutants, Water Res. 28 (1994) 1879–1889, https://doi.org/10.1016/0043-1354(94)90163-5.
[114] S.B. Bankar, M.V. Bule, R.S. Singhal, L. Ananthanarayan, Glucose oxidase — An overview, Biotechnol. Adv. 27 (2009) 489–501, https://doi.org/10.1016/j.biotechadv.2009.04.003.
[115] D.E. Edmondson, A. Mattevi, C. Binda, M. Li, F. Hubálek, Structure and mechanism of monoamine oxidase, Curr. Med. Chem. 11 (2004) 1983–1993, https://doi.org/10.2174/0929867043364784.
[116] C. Crestini, L. Jurasek, D.S. Argyropoulos, On the mechanism of the laccase-mediator system in the oxidation of lignin, Chem. Eur. J. 9 (2003) 5371–5378, https://doi.org/10.1002/chem.200304818.
[117] H. Michel, J. Behr, A. Harrenga, A. Kannt, Cytochrome c oxidase: structure and spectroscopy, Annu. Rev. Biophys. Biomol. Struct. 27 (1998) 329–356, https://doi.org/10.1146/annurev.biophys.27.1.329.
[118] E.I. Solomon, D.E. Heppner, E.M. Johnston, J.W. Ginsbach, J. Cirera, M. Qayyum, M.T. Kieber-Emmons, C.H. Kjaergaard, R.G. Hadt, L. Tian, Copper active sites in biology, Chem. Rev. 114 (2014) 3659–3853, https://doi.org/10.1021/cr400327t.
[119] M. Wikström, K. Krab, V. Sharma, Oxygen activation and energy conservation by cytochrome c oxidase, Chem. Rev. 118 (2018) 2469–2490, https://doi.org/10.1021/acs.chemrev.7b00664.
[120] S.M. Adam, G.B. Wijeratne, P.J. Rogler, D.E. Diaz, D.A. Quist, J.J. Liu, K.D. Karlin, Synthetic Fe/Cu complexes: Toward understanding heme-copper oxidase structure and function, Chem. Rev. 118 (2018) 10840–11022, https://doi.org/10.1021/acs.chemrev.8b00074.
[121] P.V. Vignais, The superoxide-generating NADPH oxidase: Structural aspects and activation mechanism, Cell Mol. Life Sci 59 (2002) 1428–1459, https://doi.org/10.1007/s00018-002-8520-9.
[122] C. Enroth, B.T. Eger, K. Okamoto, T. Nishino, T. Nishino, E.F. Pai, Crystal structures of bovine milk xanthine dehydrogenase and xanthine oxidase: structure-based mechanism of conversion, Proc. Natl. Acad. Sci. U.S.A. 97 (2000) 10723–10728, https://doi.org/10.1073/pnas.97.20.10723.
[123] D. Rehder, Metal Ion-Dependent Oxidases and Peroxidases, in: Reference Module in Chemistry, Molecular Sciences and Chemical Engineering, Elsevier, 2015. https://doi.org/10.1016/B978-0-12-409547-2.11453-2.
[124] Q. Ma, X. Zhang, Y. Qu, Biodegradation and biotransformation of indole: Advances and perspectives, Front. Microbiol. 9 (2018) 2625, https://doi.org/10.3389/fmicb.2018.02625.
[125] V.F. Ximenes, A. Campa, L.H. Catalani, The oxidation of indole derivatives catalyzed by horseradish peroxidase is highly chemiluminescent, Arch. Biochem. Biophys. 387 (2001) 173–179, https://doi.org/10.1006/abbi.2000.2228.
[126] M. Nozaki, Y. Ishimura, Chapter 16 - OXYGENASES, in: J.B. Neilands (Ed.) Microbial Iron Metabolism, Academic Press, 1974, pp. 417–444. https://doi.org/10.1016/B978-0-12-515250-1.50021-7.
[127] Y. Matoba, S. Kihara, N. Bando, H. Yoshitsu, M. Sakaguchi, K. Kayama, S. Yanagisawa, T. Ogura, M. Sugiyama, Catalytic mechanism of the tyrosinase reaction toward the Tyr98 residue in the caddie protein, PLoS Biol. 16 (2018), https://doi.org/10.1371/journal.pbio.3000077 e3000077.
[128] J.B. Broderick, Catechol dioxygenases, Essays Biochem. 34 (1999) 173–189, https://doi.org/10.1042/bse0340173.
[129] M.S. Islam, T.M. Leissing, R. Chowdhury, R.J. Hopkinson, C.J. Schofield, 2-oxoglutarate-dependent oxygenases, Annu. Rev. Biochem. 87 (2018) 585–620, https://doi.org/10.1146/annurev-biochem-061516-044724.
[130] A.R. Brash, Lipoxygenases: Occurrence, functions, catalysis, and acquisition of substrate, J. Biol. Chem. 274 (1999) 23679–23682, https://doi.org/10.1074/jbc.274.34.23679.
[131] D.E. Torres Pazmiño, M. Winkler, A. Glieder, M.W. Fraaije, Monooxygenases as biocatalysts: Classification, mechanistic aspects and biotechnological applications, J. Biotechnol. 146 (2010) 9–24, https://doi.org/10.1016/j.jbiotec.2010.01.021.
[132] A.J. Mitchell, J.K. Weng, Unleashing the synthetic power of plant oxygenases: From mechanism to application, Plant Physiol. 179 (2019) 813–829, https://doi.org/10.1104/pp.18.01223.
[133] M.J. Appel, K.K. Meier, J. Lafrance-Vanasse, H. Lim, C.-L. Tsai, B. Hedman, K.O. Hodgson, J.A. Tainer, E.I. Solomon, C.R. Bertozzi, Formylglycine-generating enzyme binds substrate directly at a mononuclear Cu(I) center to initiate O_2 activation, Proc. Natl. Acad. Sci. U.S.A. 116 (2019) 5370–5375, https://doi.org/10.1073/pnas.1818274116.
[134] M. Knop, T.Q. Dang, G. Jeschke, F.P. Seebeck, Copper is a cofactor of the formylglycine-generating enzyme, ChemBioChem 18 (2017) 161–165, https://doi.org/10.1002/cbic.201600359.
[135] T. Baysal, A. Demirdöven, Lipoxygenase in fruits and vegetables: A review, Enzyme Microbial Technol. 40 (2007) 491–496, https://doi.org/10.1016/j.enzmictec.2006.11.025.
[136] E. Carredano, A. Karlsson, B. Kauppi, D. Choudhury, R.E. Parales, J.V. Parales, K. Lee, D.T. Gibson, H. Eklund, S. Ramaswamy, Substrate binding site of naphthalene 1,2-dioxygenase: functional implications of indole binding, J. Mol. Biol. 296 (2000) 701–712, https://doi.org/10.1006/jmbi.1999.3462.
[137] E.S. Booth, J. Basran, M. Lee, S. Handa, E.L. Raven, Substrate oxidation by indoleamine 2,3-dioxygenase: Evidence for a common reaction mechanism, J. Biol. Chem. 290 (2015) 30924–30930, https://doi.org/10.1074/jbc.M115.695684.
[138] E.L. D'Antonio, E.F. Bowden, S. Franzen, Thin-layer spectroelectrochemistry of the Fe(III)/Fe(II) redox reaction of dehaloperoxidase-hemoglobin, J. Electroanal. Chem. 668 (2012) 37–43, https://doi.org/10.1016/j.jelechem.2011.12.015.
[139] G. Battistuzzi, M. Bellei, C.A. Bortolotti, M. Sola, Redox properties of heme peroxidases, Arch. Biochem. Biophys. 500 (2010) 21–36, https://doi.org/10.1016/j.abb.2010.03.002.
[140] P. Hosseinzadeh, Y. Lu, Design and fine-tuning redox potentials of metalloproteins involved in electron transfer in bioenergetics, Biochim. Biophys. Acta 2016 (1857) 557–581, https://doi.org/10.1016/j.bbabio.2015.08.006.
[141] R. Varadarajan, T. Zewert, H. Gray, S. Boxer, Effects of buried ionizable amino acids on the reduction potential of recombinant myoglobin, Science 243 (1989) 69–72, https://doi.org/10.1126/science.2563171.
[142] A.B. McKinley, C.F. Kenny, M.S. Martin, E.A. Ramos, A.T. Gannon, T.V. Johnson, S.C. Dorman, Applications of absorption spectroelectrochemistry in artificial blood research, Spectrosc. Lett. 37 (2004) 275–287, https://doi.org/10.1081/SL-120038763.
[143] S.A. Martinis, S.R. Blanke, L.P. Hager, S.G. Sligar, G. Hui Bon Hoa, J.J. Rux, J.H. Dawson,, Probing the Heme iron coordination structure of pressure-induced cytochrome P420cam, Biochemistry 35 (1996) 14530–14536, https://doi.org/10.1021/bi961511u.
[144] S.G. Sligar, Coupling of spin, substrate, and redox equilibriums in cytochrome P450, Biochemistry 15 (1976) 5399–5406, https://doi.org/10.1021/bi00669a029.
[145] S.N. Daff, S.K. Chapman, R.A. Holt, S. Govindaraj, T.L. Poulos, A.W. Munro, Redox control of the catalytic cycle of flavocytochrome P-450 BM3, Biochemistry 36 (1997) 13816–13823, https://doi.org/10.1021/bi971085s.
[146] K.L. Bren, Going with the electron flow: Heme electronic structure and electron transfer in cytochrome c, Israel J. Chem. 56 (2016) 693–704, https://doi.org/10.1002/ijch.201600021.
[147] S. Franzen, J. Belyea, L.B. Gilvey, M.F. Davis, C.E. Chaudhary, T.L. Sit, S.A. Lommel, Proximal cavity, distal histidine, and substrate hydrogen-bonding mutations modulate the activity of *Amphitrite ornata* dehaloperoxidase, Biochemistry 45 (2006) 9085–9094, https://doi.org/10.1021/bi060020z.
[148] J. Groves, Cytochrome P450 enzymes: understanding the biochemical hieroglyphs, F1000Research, 4 (2015). https://doi.org/10.12688/f1000research.6314.1.
[149] J. Zhao, J. Rowe, J. Franzen, C. He, S. Franzen, Study of the electrostatic effects of mutations on the surface of dehaloperoxidase-hemoglobin A, Biochem.

Biophys. Res. Commun. 420 (2012) 733–737, https://doi.org/10.1016/j.bbrc.2012.03.053.
[150] L.M. Carey, K.B. Kim, N.L. McCombs, P. Swartz, C. Kim, R.A. Ghiladi, Selective tuning of activity in a multifunctional enzyme as revealed in the F21W mutant of dehaloperoxidase B from Amphitrite ornata, J. Biol. Inorg. Chem. 23 (2018) 209–219, https://doi.org/10.1007/s00775-017-1520-x.
[151] I.G. Denisov, T.M. Makris, S.G. Sligar, I. Schlichting, Structure and chemistry of cytochrome P450, Chem. Rev. 105 (2005) 2253–2277, https://doi.org/10.1021/cr0307143.
[152] B. Arora, J. Mukherjee, M.N. Gupta, Enzyme promiscuity: using the dark side of enzyme specificity in white biotechnology, Sustain. Chem. Process. 2 (2014) 25, https://doi.org/10.1186/s40508-014-0025-y.
[153] A. Babtie, N. Tokuriki, F. Hollfelder, What makes an enzyme promiscuous?, Curr. Opin. Chem. Biol. 14 (2010) 200–207, https://doi.org/10.1016/j.cbpa.2009.11.028.
[154] O. Khersonsky, D.S. Tawfik, 8.03 - Enzyme promiscuity – evolutionary and mechanistic aspects, in: H.-.W. Liu, L. Mander (Eds.), Comprehensive Natural Products II, Elsevier, Oxford, 2010, pp. 47–88, https://doi.org/10.1016/B978-008045382-8.00155-6.